Redox-Active Boron Clusters

*Austin D. Ready,[a†] Yessica A. Nelson,[a†] Daniel F. Torres Pomares,[a] Alexander M. Spokoyny [a,b] **

[a] Department of Chemistry and Biochemistry, University of California, Los Angeles, 607 Charles E. Young Drive East, Los Angeles, CA 90095, USA

[b] California NanoSystems Institute (CNSI), University of California, Los Angeles, 570 Westwood Plaza, Los Angeles, CA 90095, USA

† These authors contributed equally

**Corresponding Author Information*

E-mail: spokoyny@chem.ucla.edu

Abstract/Conspectus:

In this Account, we discuss our group's research over the last decade on a class of functionalized boron clusters with tunable chemical and physical properties, with an emphasis on accessing and controlling their redox behavior. These clusters can be thought of as three-dimensional aromatic systems that have distinct redox behavior and photophysical properties than their two-dimensional organic counterparts. Specifically, our lab has studied the highly tunable, multi-electron redox behavior of $B_{12}(OR)_{12}$ clusters and applied these molecules in various settings. We first discuss the spectroscopic and electrochemical characterization of $B_{12}(OR)_{12}$ clusters in various oxidation states, followed by their use as catholytes/anolytes in redox flow batteries and chemical dopants in conjugated polymers. Additionally, the high oxidizing potential and visible light-absorbing nature of fluoroaryl-functionalized $B_{12}(OR)_{12}$ clusters have been leveraged by our group to generate weakly-coordinating, photoexcitable species which can promote photooxidation chemistry.

We have further translated these solution-phase studies on $B_{12}(OR)_{12}$ clusters to the solid state by using the precursor $[B_{12}(OH)_{12}]^{2-}$ cluster as a robust building block for hybrid metal oxide materials. Specifically, we have shown that the boron cluster can act as a thermally stable cross-linking material which enhances electron transport between metal oxide nanoparticles. We applied this structural motif to create TiO_2- and WO_3-containing materials which showed promising properties as photocatalysts and electroactive materials for supercapacitors. Building on this concept, we later discovered that $B_{12}(OCH_3)_{12}$, the smallest of the $B_{12}(OR)_{12}$ family, could retain its redox behavior in the solid state, a previously unseen phenomenon. We successfully harnessed this unique behavior for solid-state energy storage by implementing this boron cluster as the cathode-active material in a Li-ion prototype cell device. Recently, our group has also explored how to tune the redox properties of clusters other than $B_{12}(OR)_{12}$ species by synthesizing a library of vertex-differentiated clusters containing both B-OR and B-halogen groups. Due to the additive qualities of different functional groups on the cluster, these species allow access to a region of electrochemical potentials previously inaccessible by fully substituted *closo*-dodecaborate alkoxy-based derivatives.

Lastly, we discuss our research into smaller-sized redox-active polyhedral boranes (B_6- and B_{10}-based cluster cores). Interestingly, these clusters show significantly less redox stability and reversibility than their dodecaborate-based counterparts. While exploring the functionalization of *closo*-hexaborate to create fully substituted derivates (*i.e.*, $[B_6R_6H^{fac}]^-$), we observed unique oxidative decomposition pathways for this cluster system. Consequently, we leveraged this oxidative instability to generate useful alkyl boronate esters via selective chemical oxidation. We further explored a *closo*-decaborate cluster as a platform to access electrophilic $[B_{10}H_{13}]^+$ species capable of directly borylating arene compounds with unique regioselectivity. Upon chemical

oxidation of the arylated decaborate clusters, we successfully synthesized various aryl boronate esters, establishing the generality of the oxidative cluster deconstruction concept.

Overall, our work shows that boron clusters are an appealing class of redox-active molecules, and this fundamental and understudied property can be leveraged for constructing novel materials with tunable physical and electrochemical properties, as well as producing unique chemical reagents for small molecule synthesis.

Word Count: 488

Key References:

- Wixtrom, A. I.; Shao, Y.; Jung, D.; Machan, C. W.; Kevork, S. N.; Qian, E. A.; Axtell, J. C.; Khan, S. I.; Kubiak, C. P.; Spokoyny, A. M. Rapid Synthesis of Redox-Active Dodecaborane $B_{12}(OR)_{12}$ Clusters Under Ambient Conditions. *Inorg. Chem. Frontiers* **2016**, *3*(5), 711–717.[1] *Our initial report on the microwave-enabled synthesis of a library of redox-active $B_{12}(OR)_{12}$ clusters.*
- Axtell, J. C.; Messina, M. S.; Liu, J.-Y.; Galaktionova, D.; Schwan, J.; Porter, T. M.; Savage, M. D.; Wixtrom, A. I.; Rheingold, A. L.; Kubiak, C. P.; Winkler, J.R.; Gray, H.B.; Král, P.; Alexandrova, A.N.; Spokoyny, A.M. Photooxidative Generation of Dodecaborate-Based Weakly Coordinating Anions. *Inorg. Chem.* **2019**, *58*(16), 10516–10526.[2] *This paper discusses our discovery of photo-excitable $B_{12}(OR)_{12}$ clusters and the corresponding investigation of its ability to initiate olefin polymerization.*
- Mu, X.; Axtell, J. C.; Bernier, N. A.; Kirlikovali, K. O.; Jung, D.; Umanzor, A.; Qian, K.; Chen, X.; Bay, K. L.; Kirollos, M.; Rheingold, A.L.; Houk, K.N.; Spokoyny, A.M. Sterically Unprotected Nucleophilic Boron Cluster Reagents. *Chem* **2019**, *5*(9), 2461–2469.[3] *This paper details our work on the oxidative disassembly of six-membered boron clusters to cleanly generate alkly boronate esters*.
- Ready, A. D.; Irshad, A.; Kallistova, A.; Carrillo, M.; Gembicky, M.; Seshadri, R.; Narayan, S.; Spokoyny, A. M. Electrochemical Cycling of Redox-Active Boron Cluster-Based Materials in the Solid State. *J. Am. Chem. Soc.* **2023**, *145*(26), 14345–14353.[4] *Our report on the unprecedented ability of a $B_{12}(OMe)_{12}$ cluster to reversibly undergo redox transitions in the solid state.*

Introduction

Over the past century, chemists have mastered the understanding of manipulating and tuning organic molecules possessing two-dimensional aromaticity. By altering the number of aromatic rings—and thereby the extent of conjugation—chemists have learned how to deliberately engineer small molecules that can selectively interact with light. As such, there is a vast library of molecules with pronounced absorption features at different wavelengths and color intensities. Furthermore, some of these molecules can undergo well-defined photoexcitation processes upon light absorption, leading to various possible emission pathways. While many of the original discoveries in the area of manipulating organic chromophores were basic curiosities, these nevertheless have led to the development of medical[5] and commercial applications,[6-8] ranging from printable inks to electronic displays.

Two-dimensional aromaticity is not a unique delocalization phenomenon that molecules can possess. Boron clusters have been known since their original discovery in the 1950s to exhibit three-dimensional aromaticity. Surprisingly, the photophysical behavior of three-dimensional aromatic systems such as polyhedral boron clusters has been far less explored[9] than carbon-based 2D aromatic systems. Despite early phenomenological observations of colored compounds in the syntheses of small boron clusters,[10-12] no significant progress had been made with using boron clusters as building blocks for the preparation of photophysically-active molecules. One of the reasons why this area has been lagging likely stems from the photophysical inertness of many unfunctionalized boron clusters. For example, the dodecaborate cluster $[B_{12}H_{12}]^{2-}$ is a colorless white salt which, due to its large HOMO-LUMO gap (> 5 eV), does not undergo reversible electron transfer nor visible light-induced electronic excitations[13] (Figure 1A). In fact, Wiersema and Middaugh showed as early as 1967 that $[B_{12}H_{12}]^{2-}$ can only undergo a one-electron redox process

in acetonitrile at a high electrochemical potential, triggering exopolyhedral B-H functionalization chemistry, which results in the formation of a $[B_{24}H_{23}]^{3-}$ dimer. This dimer can subsequently undergo Birch reduction, resulting in the reformation of the parent $[B_{12}H_{12}]^{2-}$ cluster.[14-15] Nearly 40 years later, Peymann *et al.* discovered that upon permethylation of $[B_{12}H_{12}]^{2-}$ to give $[B_{12}(CH_3)_{12}]^{2-}$, this cluster undergoes a one-electron oxidation process to generate a blue-colored radical $[B_{12}(CH_3)_{12}]^{\bullet-}$ species.[16-17]

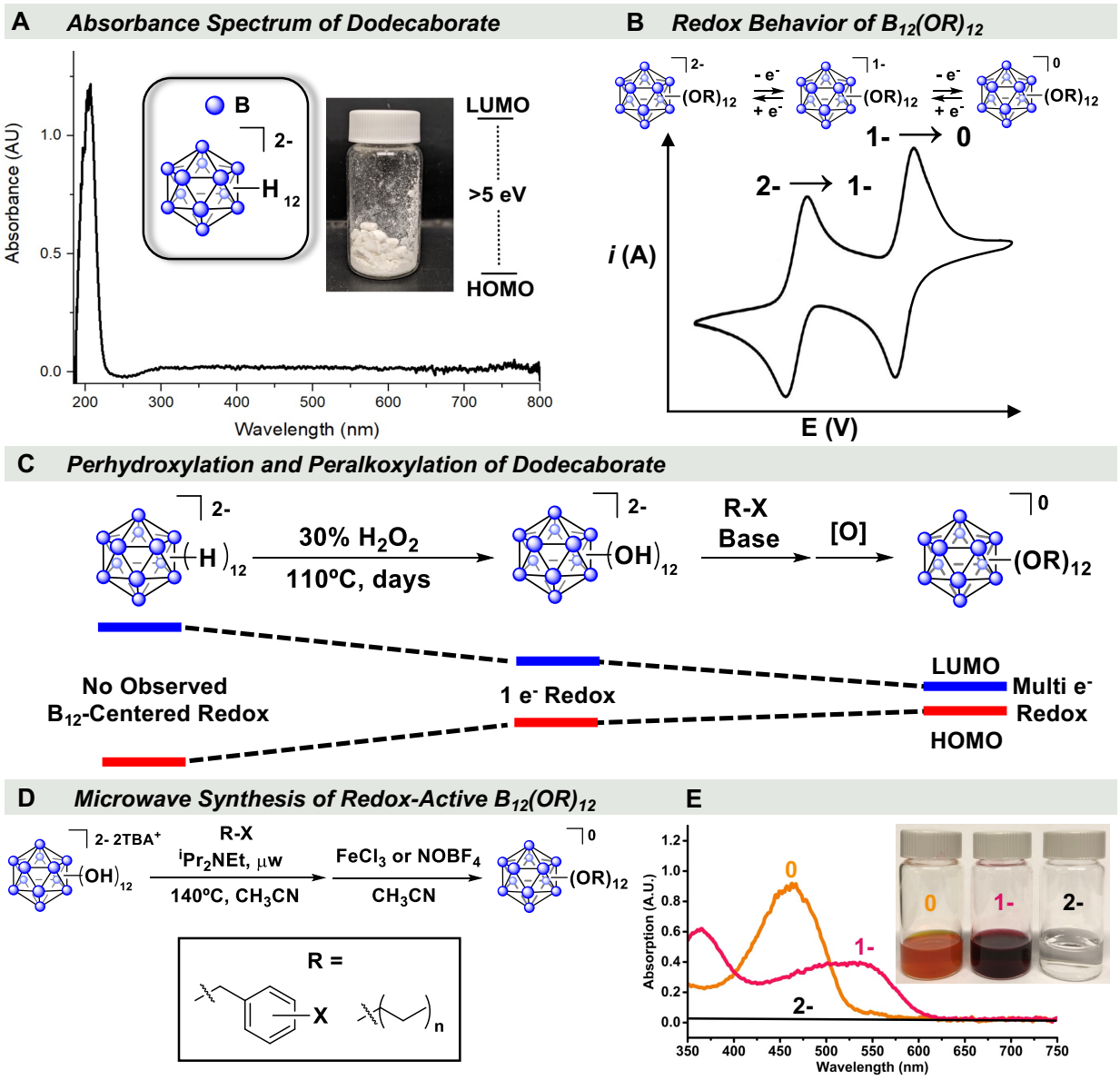

Figure 1. (A) UV-Vis absorbance spectrum of $[B_{12}H_{12}]^{2-}$ alkali salt, demonstrating its photophysical inertness. (B) Cyclic voltammogram of a representative $B_{12}(OR)_{12}$ cluster. (C) Synthetic scheme for the synthesis of $B_{12}(OR)_{12}$ clusters and simplified diagram of corresponding HOMO-LUMO gaps. (D) Representative synthesis of $B_{12}(OR)_{12}$ cluster. (E) Representative UV-Vis absorbance spectra of $B_{12}(OR)_{12}$ in different oxidation states.

In their work, the authors showed that the unpaired electron is likely delocalized on the boron cluster core, demonstrating for the first time experimentally that a B_{12}-based cluster scaffold can exhibit spin carrier properties. Shortly thereafter, it was shown that $[B_{12}H_{12}]^{2-}$ can be perhydroxylated via aggressive oxidation with 30% H_2O_2 at reflux, cleanly converting all twelve B-H vertices into B-OH groups[18-19] (Figure 1C). In doing so, the effective HOMO-LUMO gap of the cluster decreases, leading to a redox-active cluster amenable to a one-electron oxidation process.[13]

Redox-Active Boron Clusters in Solution

Importantly, numerous -OH groups on the cluster allow access to reactive handles for further cluster derivatization. Seminal work by Hawthorne *et al.* showed that deprotonation of these alcohol moieties generates nucleophilic groups capable of reacting with esters[20-21] and alkyl halides.[22-23] In particular, the reaction of $[B_{12}(OH)_{12}]^{2-}$ with alkyl halides in the presence of Hünig's base allowed the synthesis of a library of ether-functionalized $B_{12}(OR)_{12}$ clusters (Figure 1C). Notably, due to the electronic stabilization provided by the exopolyhedral -R groups, these $B_{12}(OR)_{12}$ clusters were shown to have access to two reversible electron transitions in organic solvents ($2- \rightarrow 1\bullet- \rightarrow 0$), expanding the number of known oxidation states for twelve-membered boron clusters (Figure 1B). However, these syntheses were not particularly scalable and generally required high-pressure reactors and long reaction times (days to weeks). Therefore, our group set out to improve on this chemistry by using a microwave-assisted method, allowing milder syntheses of numerous $B_{12}(OR)_{12}$ clusters in minutes/hours, without the need for air-free conditions or

rigorously dried solvents[1] (Figure 1D). Importantly, this simple and scalable method enabled the synthesis of some of these species on a multigram scale, a prerequisite to further exploring their materials-relevant chemistry and photophysical properties.

In sharp contrast to the parent $[B_{12}H_{12}]^{2-}$ cluster, $B_{12}(OR)_{12}$ species can be isolated in numerous oxidation states through chemical oxidants/reductants and column chromatography, enabling access to a class of potent chromophores. ^{11}B NMR spectroscopy is a diagnostic tool to conveniently detect these oxidation state changes (Figure 2B). Specifically, the cluster shows a dramatic change in the chemical shift from -20 ppm (2-) to +40 ppm (neutral), whereas the cluster is spectroscopically silent in the 1- state due to its radical anionic nature. Importantly, the clusters in the radical anionic and neutral states exhibit pronounced colorations due to strong absorptions in the visible light region (Figure 1E), ranging in color from red to pink to orange.[1,23-25]

Consistent with the oxidation processes occurring primarily on the boron cluster core, X-ray photoelectron spectroscopy provides diagnostic evidence for these changes, wherein the binding energy of B 1s electrons shifts to higher values (eV) as the cluster is oxidized from 2- to 1- (Figure 2A), corresponding to the decreasing electron density of the cluster core. Despite being spectroscopically silent by ^{11}B NMR spectroscopy, the paramagnetic radical anion is visible by electron paramagnetic resonance (EPR) spectroscopy (Figure 2E), with time-dependent density-functional theory (TD-DFT) calculations (inset) on the singly occupied molecular orbital (SOMO) showing the electron density localized on the cluster core. The vast number of possible couplings between the unpaired electron and each boron atom in the cluster manifests as a broad EPR signal without observable hyperfine couplings, further supporting the core-delocalized nature of the radical anion.[1,13,26]

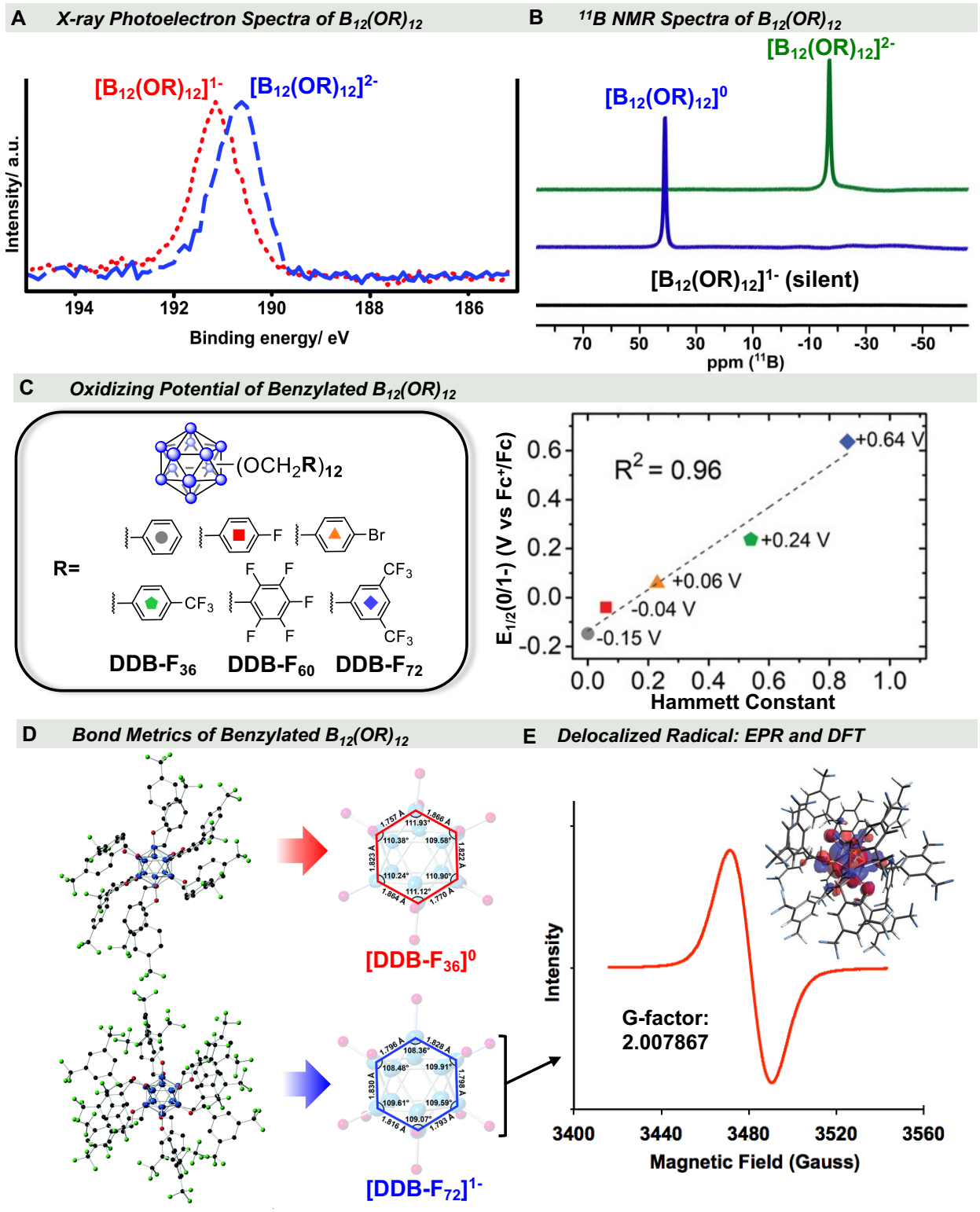

Figure 2. (A) – (E) Select characterization and spectroscopic data for $B_{12}(OR)_{12}$ clusters in 2-/1- oxidation states. Figure adapted from ref (1) with permission from the Chinese Chemical Society (CCS), Peking University (PKU), and the Royal Society of Chemistry. Figure 2C adapted from ref (28) with permission. Copyright 2020 WILEY-VCH Verlag GmbH & Co. KGaA, Weinheim.

Oxidation processes can also be observed from the structural changes occurring on the B_{12}-based cluster core. For example, $[B_{12}(OR)_{12}]^{2-}$ exists as a perfect icosahedron, with nearly identical B-B distances throughout the cluster. However, as the cluster is subsequently oxidized to 1- and then 0, the crystal structure shows increasing distortions as the electron density in the cluster decreases (Figure 2D). Average B-B bond lengths increase, and the overall range of distances broadens upon oxidation. Additionally, the average B-O bond lengths shorten, along with B-B-B angle distortions.[1,22]

The electrochemical potential of these electronic transitions is highly dependent on the electron-donating/-withdrawing nature of the -R substituents, with a range of potentials covering 1.2 V.[25] We have further expanded on this work by synthesizing a number of new derivatives containing highly electron-withdrawing fluorinated benzyl groups, pushing the upper boundaries of the electrochemical potential window for these clusters to +0.2 to +0.6 V vs Fc^+/Fc (Figure 2C). Notably, we showed that the attachment of a 3,5-bis(trifluoromethyl)benzyloxy substituent to each boron vertex creates a powerful dodecaborane oxidant (DDB-F_{72}) due to the 72 electron-withdrawing fluorine atoms present around the cluster periphery. In fact, DDB-F_{72} has a lower-lying LUMO than the popular p-type dopant F_4TCNQ (2,3,5,6-tetrafluoro-7,7,8,8-tetracyanoquinodimethane), making it ~ 0.5 V more oxidizing (Figure 3A). As such, various benzylated $B_{12}(OR)_{12}$ clusters—especially the fluorinated derivatives (DDB-F_{36}, DDB-F_{60}, and DDB-F_{72})—can act as exceptional molecular dopants in a P3HT (poly(3-hexylthiophene-2,5-diyl)) conjugated polymer[27-28] (Figure 3). Upon removing an electron from the polymer backbone, $[DDB\text{-}F_{72}]^-$ does not form a strong electrostatic attraction with the resulting polaron, which is an important prerequisite for high carrier mobility. More recently, this has been expanded to semiconducting single-walled carbon nanotubes (s-SWCNT) (Figure 3B).[29-30] The dopant

character of $[DDB\text{-}F_{72}]^-$ is attributed to the large steric profile of the substituents and the core-localized nature of the electron density. Conceptually, these fluorinated clusters can be considered redox-active weakly coordinating anions (WCAs).

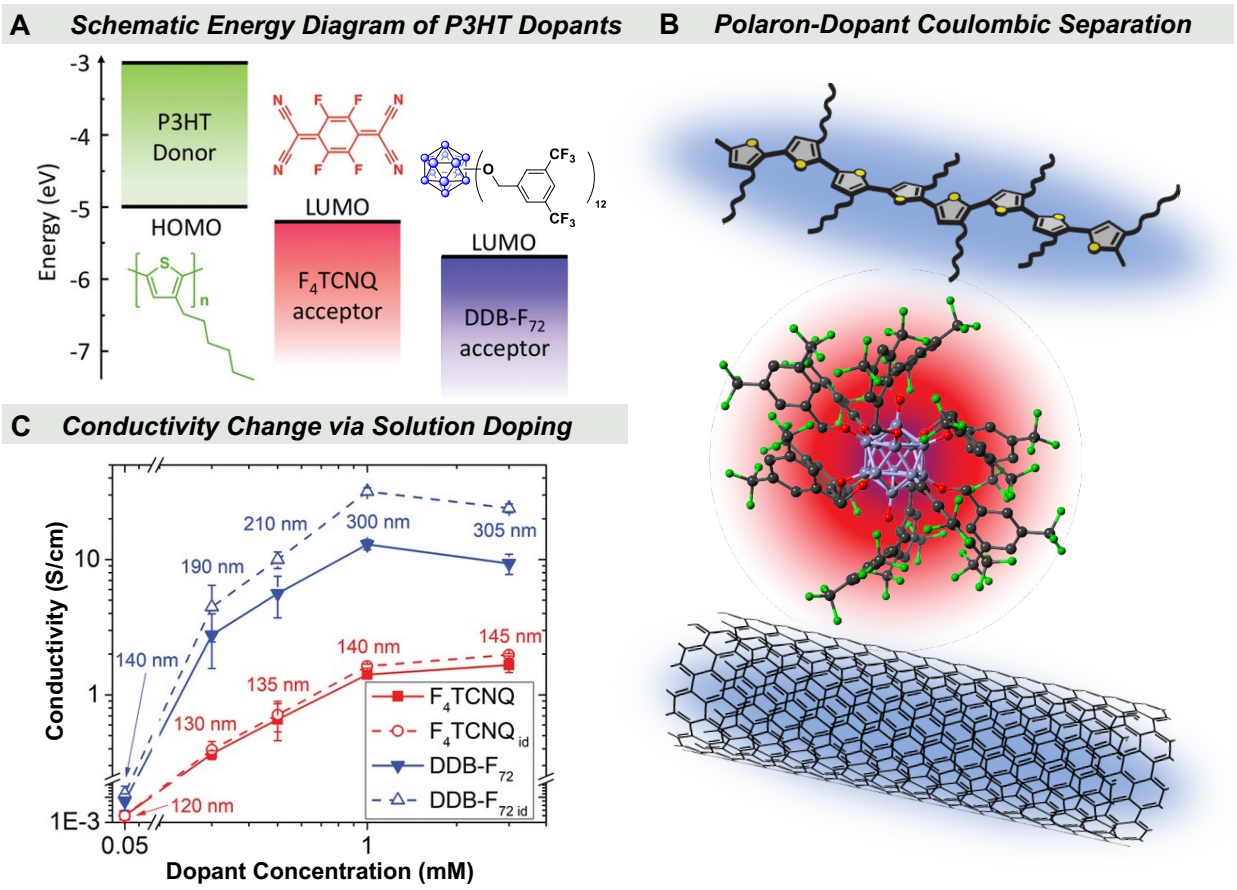

Figure 3. (A) Schematic energy diagram of P3HT HOMO vs F_4TCNQ and $[DDB\text{-}F_{72}]^0$ LUMOs. (B) Cartoon of $DDB\text{-}F_{72}$ doping a P3HT polymer (top) and s-SWCNT (bottom). (C) P3HT conductivity as a function of dopant concentration. Figure 3C adapted from ref (27) with permission. Copyright 2019 WILEY-VCH Verlag GmbH & Co. KGaA, Weinheim.

Fluorinated benzyloxy derivatives of dodecaboranes are not only potent oxidants and WCAs (Figure 3B), but their chromophoric nature engenders access to electronic excitations with visible light. As such, we showed that $[B_{12}(OR)_{12}]^0$ clusters with varying amounts of fluorination (*i.e.*, $DDB\text{-}F_{36}$, $DDB\text{-}F_{60}$, and $DDB\text{-}F_{72}$) can, upon irradiation with blue light, access a highly oxidizing photoexcited state (Figure 4A) which promotes small molecule oxidation to initiate the

controllable polymerization of a number of styrene and other olefin derivatives.[2,31] Importantly, the previously established weakly coordinating nature of the resulting $[B_{12}(OR)_{12}]^{1-}$ species prevents incorporation into the resulting polymer via chain termination processes. DFT studies on DDB-F_{60} suggest that an electron from a lower-lying orbital on an aryl ring is promoted via visible light to a cluster-based LUMO to generate the excited state (Figure 4B).

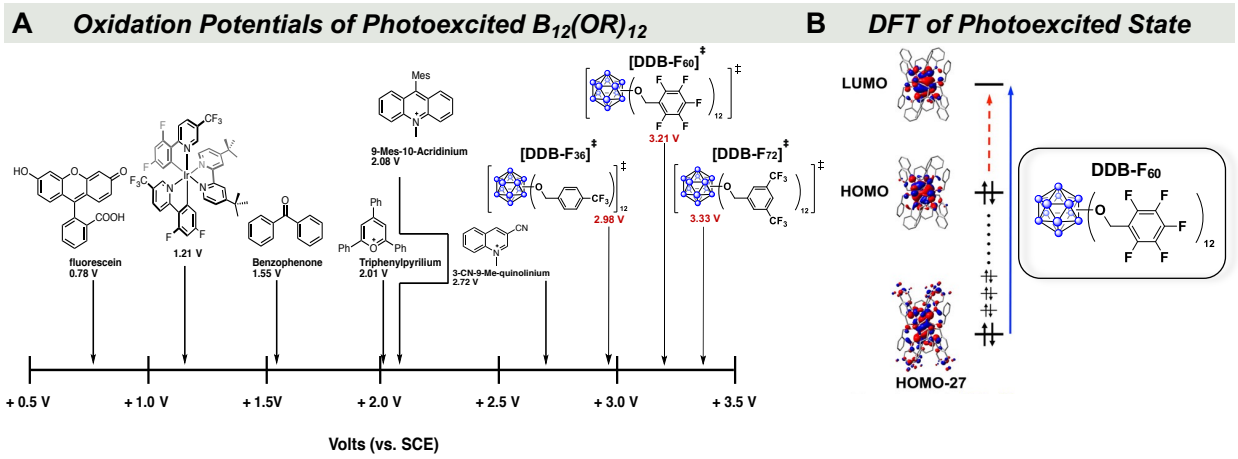

Figure 4. (A) Oxidation potentials of photoexcited $B_{12}(OR)_{12}$ clusters (calculated) with respect to several traditional photooxidants. (B) Molecular orbital diagram corresponding to the photoexcitation of DDB-F_{60}. Figure 4B adapted with permission from ref (31). Copyright 2016 American Chemical Society.

Additionally, we showed that DDB-F_{60} and several other clusters bearing pentafluoroaryl motifs are amenable to post-modification via S_NAr chemistry, leading to redox-active clusters with modifiable peripheries. Using this strategy, we prepared a family of atomically precise nanoparticle molecules (2-5 nm) and used these constructs to efficiently bind to proteins in a multivalent fashion.[32] Similarly, we later showed that clusters terminated with iodoarene moieties can be easily converted into permetallated Au(III) nanomolecules, efficiently reacting with various thiols under aqueous conditions. This work demonstrated that redox-active boron clusters can

serve as stable, rigid, atomically precise scaffolds which are mimics of traditional covalent gold nanoparticles.[33]

Considering that the redox events observed for the $B_{12}(OR)_{12}$ system via cyclic voltammetry exhibit well-defined reversible and tunable properties, we explored using this cluster system for electrochemical energy storage. We leveraged the ability of $B_{12}(OR)_{12}$ compounds to span a breadth of electrochemical potentials by constructing a full redox flow battery (RFB) (Figure 5A) containing different R-substituted clusters as both the catholyte and anolyte.[34] DDB-F_{72} [1] was chosen for its high oxidation potential ($E_{1/2}$ = 0.07 V vs Fc^+/Fc; 2-⟶1-) relative to the reduction potential of [2] ($E_{1/2}$ = -0.26 V vs Fc^+/Fc; 0⟶1-), an electron-rich alkoxylated derivative. These clusters showed excellent stability upon 45 days of electrochemical cycling, with no apparent cluster degradation (Figure 5A), establishing the viability of $B_{12}(OR)_{12}$ clusters for electrochemical energy storage systems.

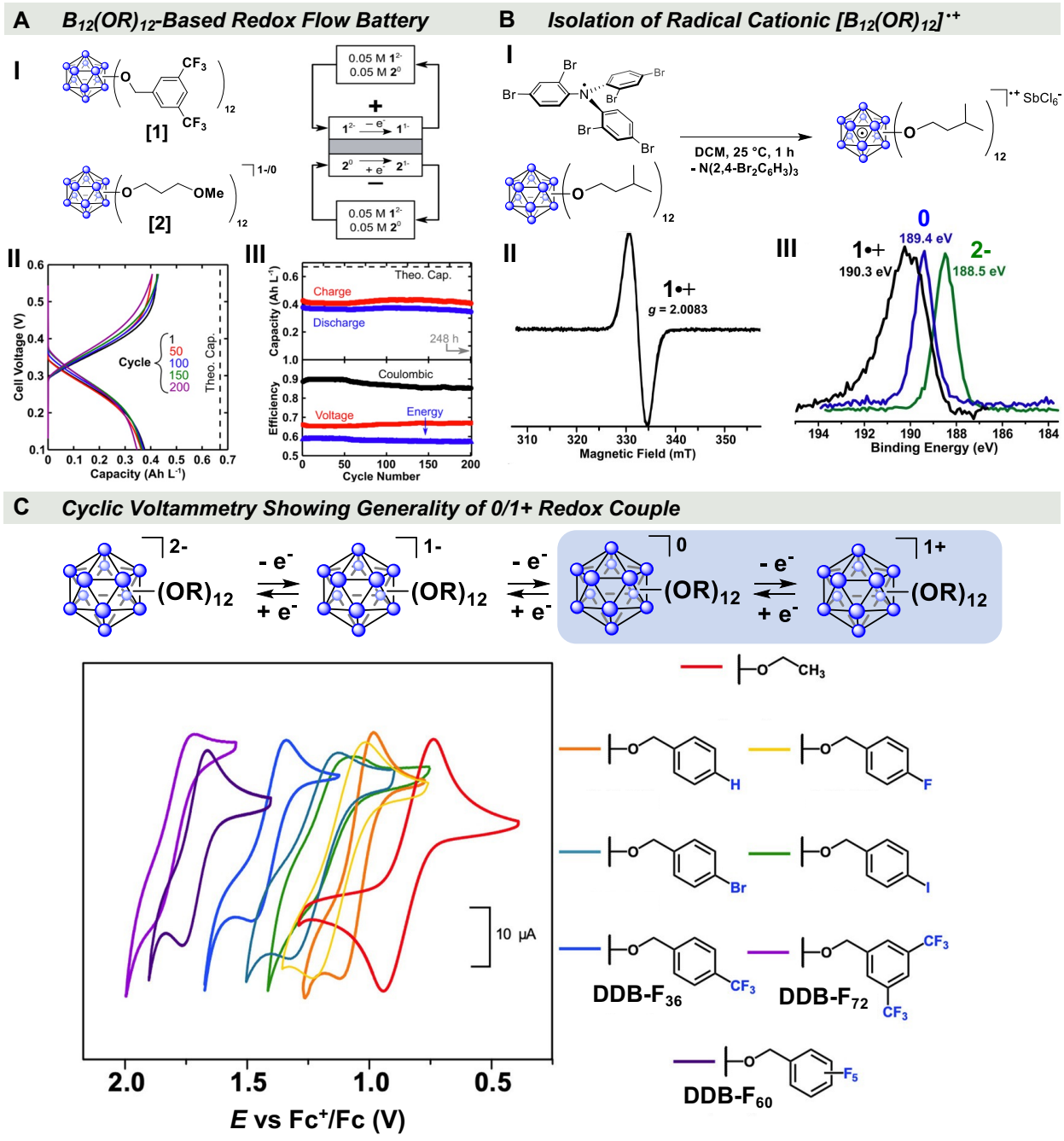

Figure 5. (A) $B_{12}(OR)_{12}$ cluster used in redox flow batteries. (B) – (C) Synthesis and spectroscopic characterization of the radical cluster cations including $[B_{12}(O\text{-}3\text{-methylbutyl})_{12}]^{\bullet+}$. Figure 5A, adapted from ref (34), Figure 5B adapted from ref (35), and Figure 5C adapted from ref (36) with permission. Copyright 2019-2021 American Chemical Society.

On the opposite end of the electrochemical potential window, we hypothesized that the stabilization provided by highly electron-donating alkyl substituents on the boron cluster could engender access to an additional super-oxidized cationic state. To probe this concept, we synthesized the B_{12}(O-3-methylbutyl)$_{12}$ cluster and, via cyclic voltammetry, identified a previously undiscovered radical cationic state.[23] This cationic boron cluster can be isolated in the +1 state via oxidation with a potent triarylaminium oxidant (Figure 5B). Spectroscopic characterization of $[B_{12}(O\text{-}3\text{-}methylbutyl)_{12}]^{+\bullet}$, including EPR (Figure 5B) and XPS (Figure 5B) spectra, are consistent with the proposed radical cationic nature of this compound. This discovery led us to reexamine the electrochemical behavior of other $B_{12}(OR)_{12}$ clusters, revealing that many of these species also have access to this additional super-oxidized state (Figure 5C).

This expanded the known oxidation states of $B_{12}(OR)_{12}$ systems to four in total[35-36] and was the first example of a cationic dodecaborane cluster. ENDOR (Electron Nuclear Double Resonance) spectroscopy was further utilized successfully to corroborate the weak hyperfine couplings of these radical $B_{12}(OR)_{12}$ species.[26]

Boron Clusters in the Solid-State

We hypothesized that because of the harsh oxidizing conditions required to synthesize the parent $[B_{12}(OH)_{12}]^{2-}$ cluster (30% H_2O_2, reflux), this chemical robustness could be leveraged by using this compound as a molecular scaffold for hybrid inorganic materials, especially ones that require extreme oxidizing conditions during their syntheses. In particular, many metal oxides require thermal annealing at elevated temperatures under an atmosphere of oxygen.

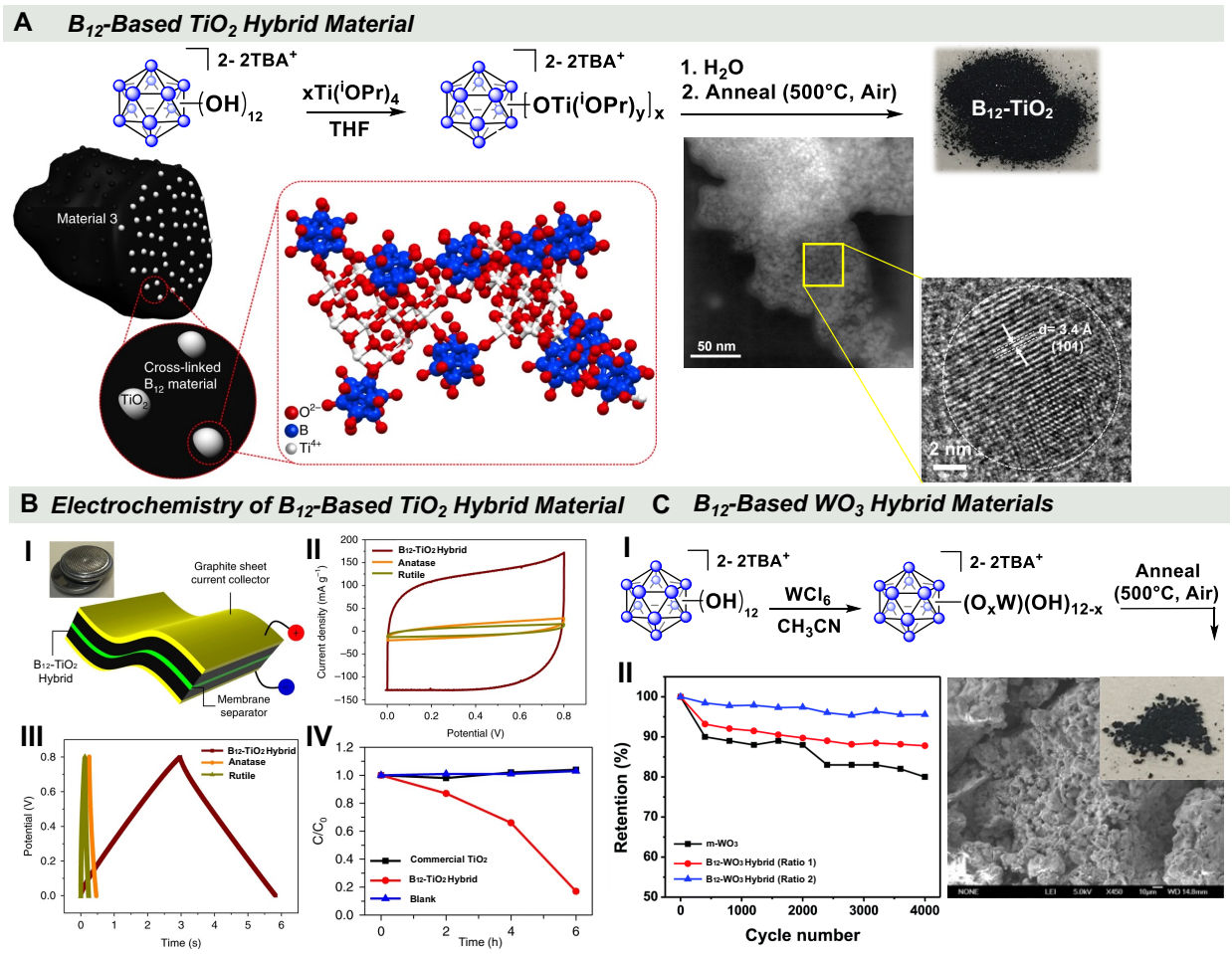

Figure 6. (A) – (C) Use of $[B_{12}(OH)_{12}]^{2-}$ as a redox-active cross-linker for hybrid metal oxide materials. Figure 6B adapted from ref (37) and Figure 6C adapted from ref (38) with permission from the Royal Society of Chemistry and Springer Nature.

To test our hypothesis, we included a $[B_{12}(OH)_{12}]^{2-}$ precursor as a component in the classical workflow of the sol-gel synthesis of titania nanoparticles.[37] In the last step, the gel material was annealed at 500 °C in air, and the hybrid product was subjected to various characterization methods. Through a combination of techniques, including powder X-ray diffraction (PXRD), electron microscopy, XPS, and solid-state ^{11}B NMR, this material was concluded to be a cross-linked hybrid between small titania nanoparticles (< 10 nm) and intact boron clusters (Figure 6A). Importantly, we observed the presence of B-O-Ti linkages by multiple

spectroscopic techniques, corroborating the structural interface of this material (Figure 6A). This B_{12}-based-TiO_2 hybrid material showed promise as both an active-layer component in a pouch-cell supercapacitor (Figure 6B) and as a photocatalyst for the visible-light-induced decomposition of aqueous organic contaminants, outperforming the anatase and rutile phases of pure TiO_2 (Figure 6B). The cross-linked network morphology enabled by intact boron clusters resulted in improved electron transfer rates, electronic conductivities, and light-absorption abilities compared to pure TiO_2.

Having established the utility of $[B_{12}(OH)_{12}]^{2-}$ as a cross-linking agent for metal oxide nanoparticles, we further explored this concept by synthesizing a B_{12}-based hybrid tungsten oxide material via a WCl_6 precursor in combination with $[B_{12}(OH)_{12}]^{2-}$ (Figure 6C). When used as a supercapacitor electrode, this cross-linked material showed enhanced cycling stability at different stoichiometric ratios of boron cluster compared to monoclinic, pristine tungsten oxide[38] (Figure 6C). The extensive cross-linking present in the B_{12}-based tungsten oxide materials both improves conductivity and acts as a mechanical support for the metal oxide nanoparticles, reducing structural degradation caused by electrochemical cycling.

These studies showcased the potential of $[B_{12}(OH)_{12}]^{2-}$ as a building block for extended solids, with promising applications in energy storage. However, the titanium/tungsten oxide materials showed long-range disorder due to the amorphous boron-cluster-containing regions connecting the crystalline metal oxide nanocrystals. Consequently, we hypothesized that a more ordered, crystalline boron-cluster-based composite could allow access to unique solid-state electrochemical applications. Particularly, we envisioned that a boron-cluster-based electrode material could be realized if the boron cluster itself could undergo redox in the solid state, in contrast to the use of redox-inert dodecaborate cluster derivatives for solid-state electrolytes.[39] We

therefore returned to the $B_{12}(OR)_{12}$ clusters as a platform to investigate this due to their multi-electron, highly reversible redox behavior, and synthetic tunability. To investigate whether the solution-phase redox behavior of $B_{12}(OR)_{12}$ could be retained in the solid state—a previously unreported phenomenon—we identified $B_{12}(OCH_3)_{12}$ as an ideal candidate due to its relatively low molecular weight, high crystallinity as a bulk solid, and sterically-accessible ether oxygens. We developed a microwave-assisted synthesis of this cluster using trimethyl sulfonium bromide as a methylating reagent, followed by an aqueous Ce(IV) oxidation (Figure 7A). Surprisingly, when a model solid-state Li-ion cell was constructed with $[B_{12}(OCH_3)_{12}]^0$ as the active cathode material in a poly(ethylene oxide) (PEO) matrix (Figure 7B) and cycled at 60 °C, a reversible one-electron event was observed in the solid-state cyclic voltammogram at 3.45 V vs Li^+/Li, which we attributed to the $[B_{12}(OCH_3)_{12}]^0/[B_{12}(OCH_3)_{12}]^{1-}$ redox couple[4] (Figure 7C).

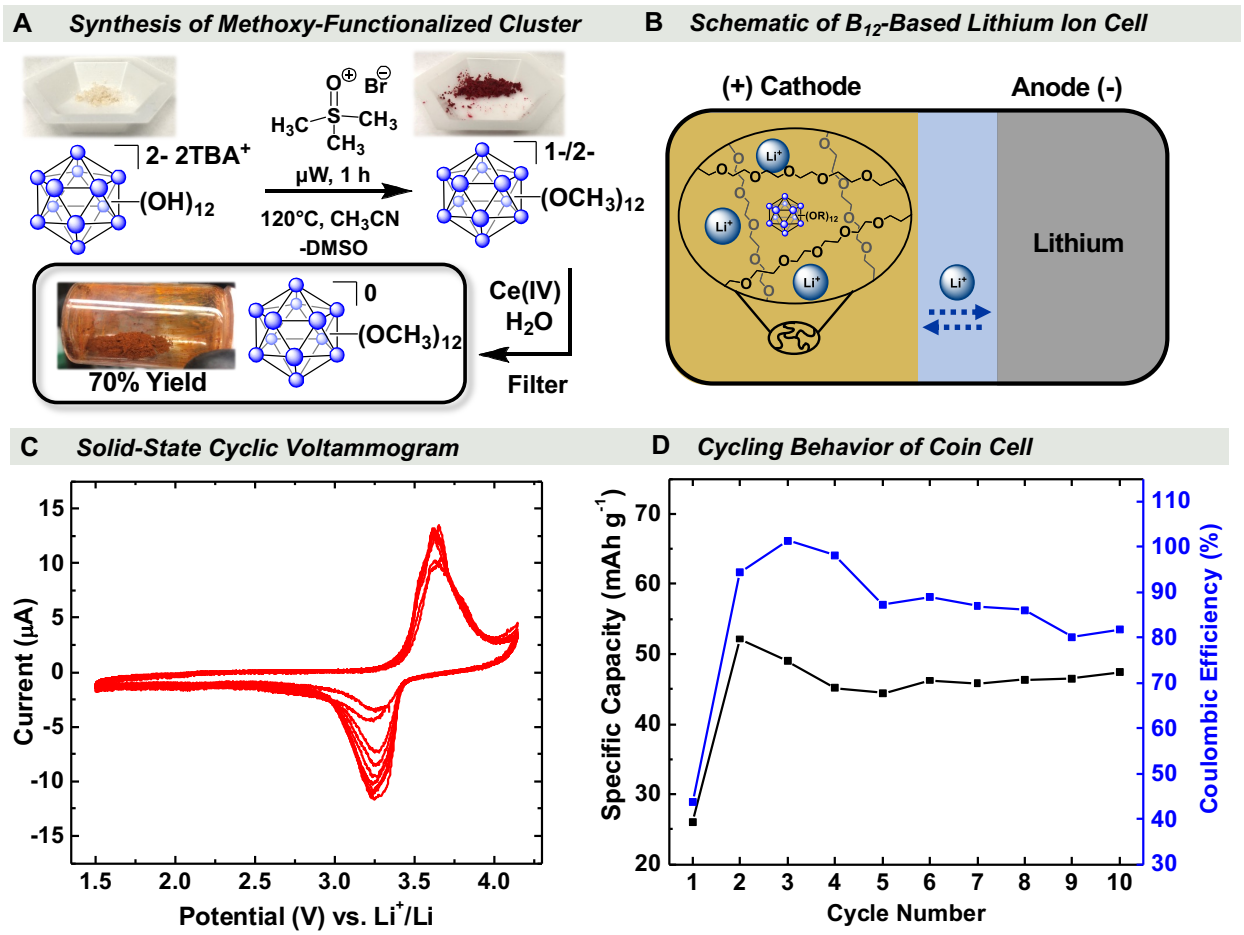

Figure 7. (A) Microwave synthesis of $[B_{12}(OCH_3)_{12}]^0$ and (B) – (D) its use as a cathode-active material. Figure 7(C) – (D) adapted with permission from ref (4). Copyright 2023 American Chemical Society.

This work represents the first example of a boron cluster undergoing reversible redox in the solid state, and the high Coulombic efficiency and cycling stability (Figure 7D) further supported this new approach to utilizing these clusters for energy storage applications. Additional improvements to the energy storage capacity of these materials could conceivably be achieved by incorporating additional redox-active cations or using lighter polyhedral boron clusters.

Vertex-Differentiated Boron Clusters

As we investigated the effects of vertex differentiation at multiple sites on *closo*-dodecaborate, we explored how introducing halogens as electron-withdrawing groups impacts the

cluster's chemical properties. Perhalogenated clusters ($[B_{12}X_{12}]^{2-}$ X= Cl, Br) were shown in early reports to display redox activity at exceptionally high potentials[40] (> +2 V vs. Fc^{+}/Fc). The high redox potentials of these clusters provide a contrast to our studies of redox-active species containing exclusively -OR groups[1] (Figure 8A). Intrigued by the possibility of modulating oxidation potentials by vertex differentiation and harnessing the inherent stabilities of the clusters inferred from the B-H halogenation, we hypothesized that a broader range of redox potentials could be achieved through a mixed functionalization strategy.

Inspired by Peymann *et al*.'s work on the sequential acid-catalyzed hydroxylation of the $[B_{12}H_{12}]^{2-}$ cluster,[42] we systematically worked to find the optimal conditions to exclusively synthesize the trihydroxylated $[B_{12}H_9(OH)_3]^{2-}$ cluster on a multigram scale. The synthesis of this cluster occurs in a regioselective fashion, exclusively producing a 1,7,9-substituted trihydroxylated cluster. Once the trihydroxylated cluster is isolated, perhalogenation can be employed to functionalize the remaining B-H vertices.

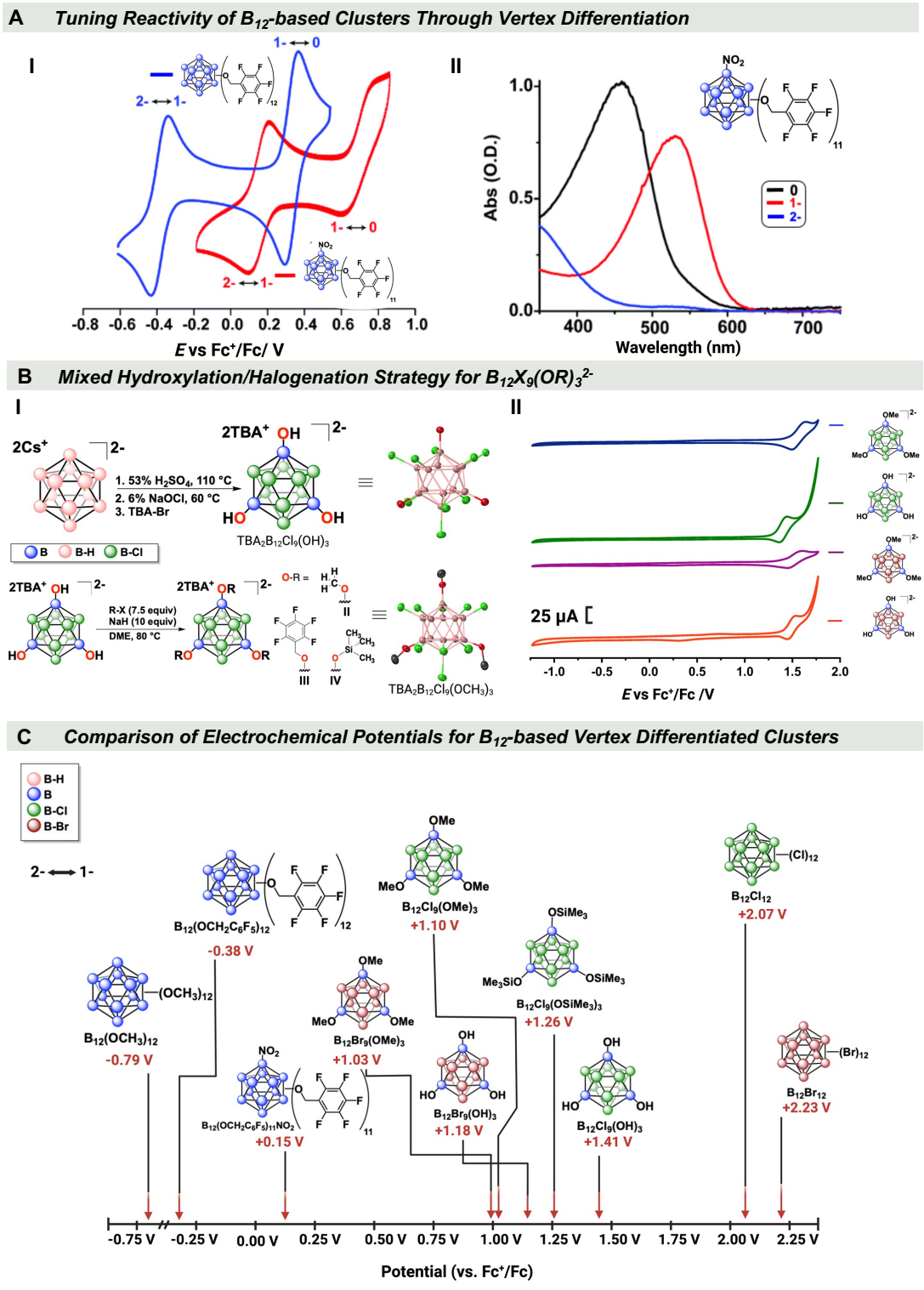

Figure 8. (A) – (C) Vertex differentiated functionalization of dodecaborate-based clusters leads to tunable redox properties. Figure 8A adapted from ref (24) and Figure 8B adapted from ref (41) with permission. Copyright 2018-2023 Royal Society of Chemistry and American Chemical Society, respectively.

To accomplish this, sodium hypochlorite can be used as an aqueous chlorinating reagent for the $[B_{12}H_9(OH)_3]^{2-}$ anion, producing the $[B_{12}Cl_9(OH)_3]^{2-}$ species[41] (Figure 8B). Similarly, the perbrominated analogue $[B_{12}Br_9(OH)_3]^{2-}$ can be synthesized from an aqueous solution of $[B_{12}H_9(OH)_3]^{2-}$ and Br_2 in methanol. The -OH groups on the perhalogenated systems are amenable to functionalization by a range of electrophiles, despite the surrounding bulky halogens. These hydroxyl moieties can undergo alkylation, benzylation, and silylation (Figure 8B). Vertex-differentiated clusters displayed a reversible one-electron redox event assigned to the 2−/1− couple, with an $E_{1/2}$ ranging from +1.03 V to +1.41 V vs. Fc^+/Fc (Figure 8B). These vertex-differentiated clusters showed chemical oxidation at higher potentials than their $[B_{12}(OR)_{12}]^{2-}$ analogues but lower potential than the corresponding perhalogenated species, highlighting the additive effect of mixing different functional groups on the B_{12}-based cluster core.

The perfunctionalized $Li_2B_{12}Cl_{12}$ and $Li_2B_{12}(OH)_{12}$ clusters undergo a polymorphic transition induced by heat, facilitating the reorientation of cations in the lattice.[39,43] This reorientation enables solid-state ionic conductivity. We investigated if the vertex-differentiated clusters could retain this attribute and potentially enhance it. Initially, we postulated that the modified vertex-differentiated clusters would create more vacancies in the crystal lattice, potentially resulting in increased solid-state ionic conductivity at room temperature. Despite lower ionic conductivities of the trihydroxylated/halogenated clusters at room temperature, we were surprised that the ionic conductivities are comparable to that of the $[B_{12}OH_{12}]^{2-}$ system at high temperatures (> 200 °C), pointing to the presence of vacancies likely not being the dominant parameter governing this property.[44] Interestingly, $[B_{12}Cl_9(OH)_3]^{2-}$ displays remarkable thermal stability by thermogravimetric analysis (TGA), with decomposition onset surpassing 500 °C,

opening possible uses for these systems as weakly coordinating anions under high-temperature conditions.

Our investigation into $B_{12}(OR)_{12}$ clusters and related systems unveiled remarkable metal-like redox processes observed for many perfunctionalized compounds. Consequently, we wondered whether this phenomenon was generalizable to other boron-only cluster systems. We initially concentrated on the smaller-sized *closo*-$[B_6H_6]^{2-}$ species,[45] primarily because the functionalization and applications of this cluster were significantly underexplored. Prompted by our previously reported microwave-assisted technique for attaching alkyl groups to $[B_{12}(OH)_{12}]^{2-}$, we explored whether this method could also be applied to create fully persubstituted B_6-based compounds. During our investigations, we discovered that reacting $[B_6H_6H^{fac}]^-$ with an excess of benzyl bromide and Hünig's base in acetonitrile under microwave heating can produce a persubstituted cluster[46] (Figure 9A). Optimization of these conditions enabled the isolation of $[B_6(CH_2C_6H_5)_6H^{fac}]^-$, an air- and moisture-stable solid at room temperature. This compound's electrochemical characterization showed an irreversible oxidation, suggesting possible cage degradation. Importantly, this reactivity profile is distinct from the fully alkylated dodecaborate $[B_{12}(CH_3)_{12}]^{2-}$, which exhibited a reversible single-electron oxidation, leading to the formation of $[B_{12}(CH_3)_{12}]^{\bullet-}$.[16] In contrast, the CV of $[B_6(CH_2C_6H_5)_6H^{fac}]^-$ (**1a)** in CH_3CN (Figure 9B, I) at faster scan rates reveals the pseudoreversibility of the redox couple. This electrochemical behavior does not significantly change when variations are made to the benzyl substituents, as demonstrated by $[B_6(CH_2\text{-}4\text{-}Br\text{-}C_6H_4)_6H^{fac}]^-$ (**1b**). The decomposition of compounds **1a** and **1b** under oxidizing electrochemical potentials is consistent with the removal of an electron from the cluster-based HOMO, resulting in kinetic destabilization due to a disruption of three-dimensional aromaticity (Figure 9).

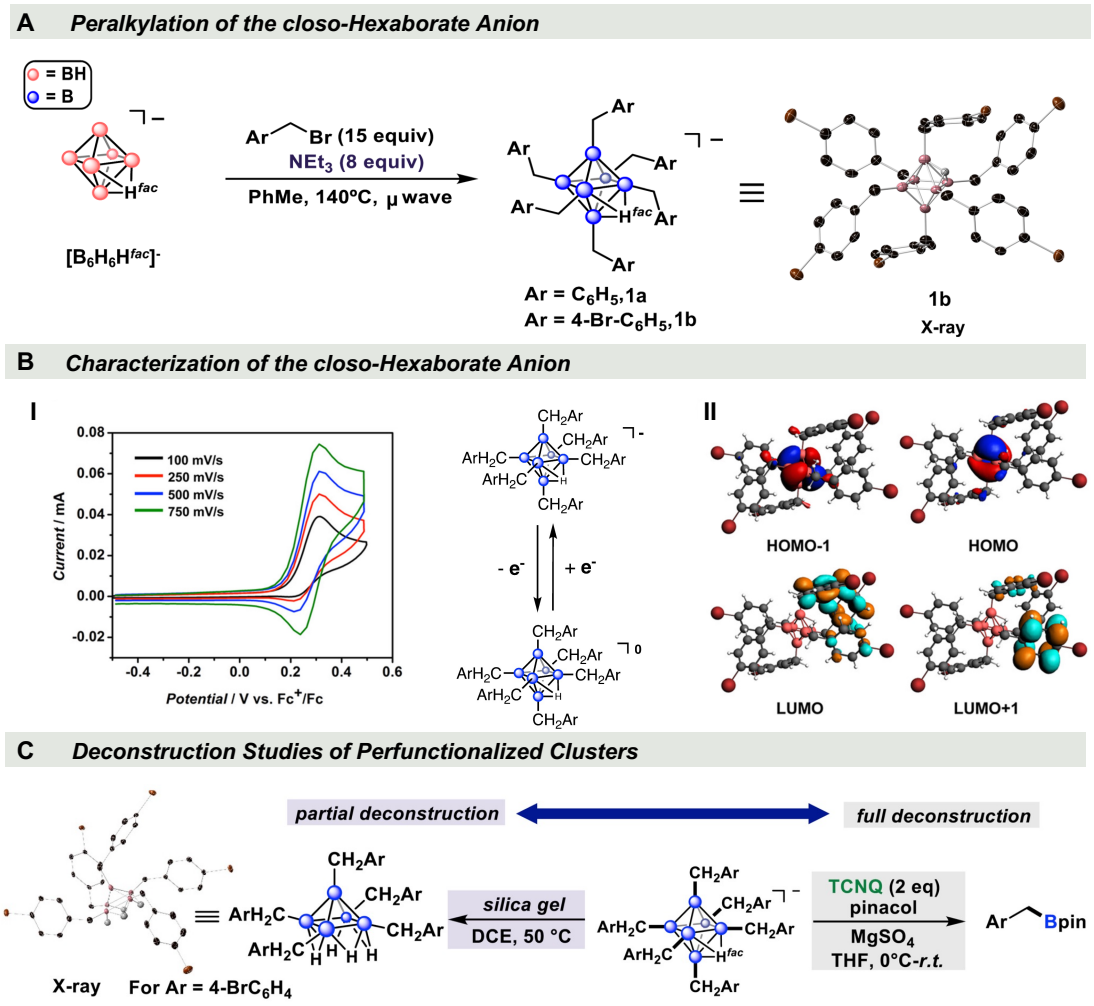

Figure 9. (A) - (C) Development of the nucleophilic borylation strategy using inherent redox activity of the functionalized B_6-based clusters. Figure 9A and 9C adapted from ref (3) and Figure 9B adapted from ref (36) with permission. Copyright 2017-2019 American Chemical Society and Elsevier, respectively.

In the process of purifying **1b**, we observed through multinuclear NMR spectroscopic analysis the formation of a new cluster-based species upon exposure to silica gel, indicative of a partial cage disassembly[3] (Figure 9C). This species was identified by notable shifts in the ^{11}B NMR spectra, which indicated a loss of symmetry relative to the original perfunctionalized cluster. ^{1}H NMR spectroscopy confirmed the emergence of new bridging hydrides, along with the loss of a 'B–CH_2Ar' vertex from the initial cluster (Figure 9C). We investigated ways of leveraging this partial cage deconstruction to achieve the selective degradation of the fully substituted $[B_6R_6H^{fac}]^-$

clusters using chemical oxidants. Controlled degradation of $[B_6R_6H^{fac}]^-$ compounds allowed mononuclear alkyl boronate products to be isolated. To improve this process further, we revised our synthetic strategy and used the dianionic $[B_6H_6]^{2-}$ cluster without the H^{fac} site. This allowed us to facilitate a base-free nucleophilic substitution of various electrophiles (Figure 10), forming monoalkylated B_6-based clusters with comparable oxidation potentials. Mono-substituted B_6-based clusters can then undergo efficient oxidative deconstruction using simple oxidants, which furnish alkyl boronate esters in the presence of pinacol (Figure 10).

The B_6-based cluster system successfully provided a new route toward the formation of mononuclear alkyl boronates, and we wondered whether we could establish a similar approach for the aryl-based congeners. Unfortunately, reactivity studies engaging $[B_6H_6]^{2-}$-based nucleophiles in nucleophilic aromatic substitution chemistry with activated arene electrophiles have so far proven futile in our laboratory. Therefore, we focused on a different approach where a boron cluster can exhibit electrophilic reactivity, activating C-H bonds in arenes. Hawthorne previously demonstrated that $[B_{10}H_{10}]^{2-}$ undergoes an acid-induced cage-opening, postulating formation of a reactive intermediate ($[B_{10}H_{13}]^+$).[47-48] We theorized that if this reactivity of the B_{10}-based cluster could be expanded to a variety of substituted arenes, this could be followed by a selective deconstruction process to synthesize aryl boronic esters (Figure 11A).

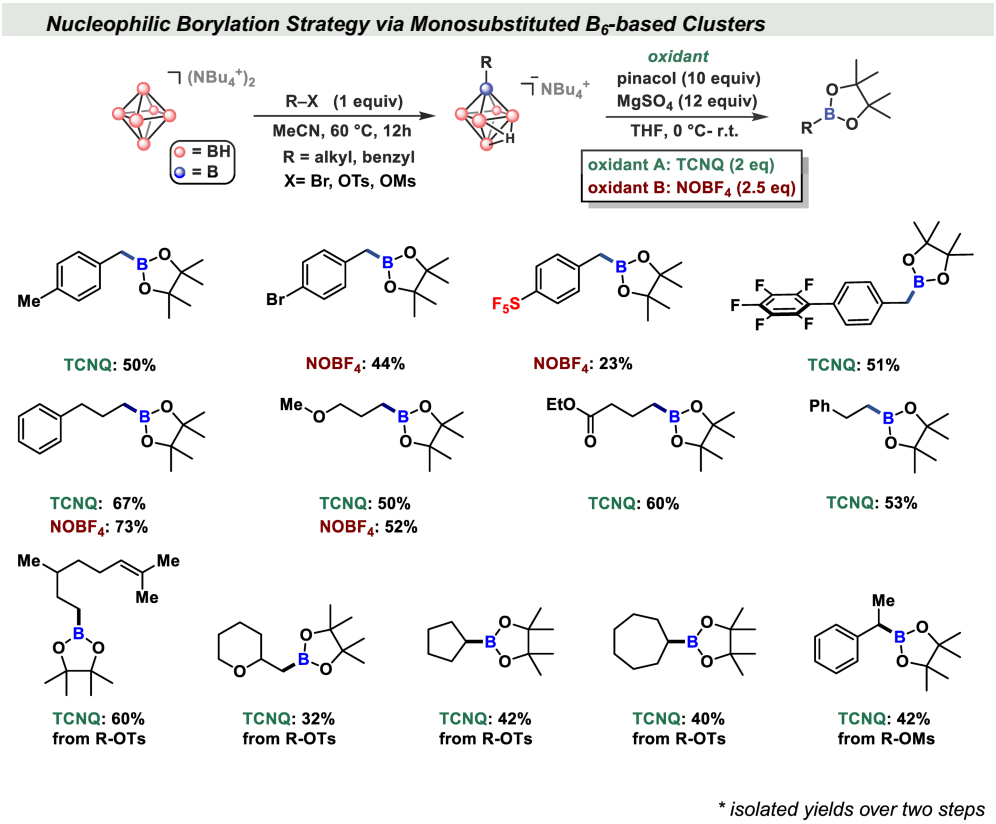

Figure 10. Use of $[B_6H_6]^{2-}$ cluster as a nucleophilic borylation reagent. Isolated yields are calculated after cage deconstruction.

As part of our investigation, we discovered that for B_{10}-based clusters, we needed to use the oxidant CAN (cerium(IV) ammonium nitrate) instead of the previous hexaborate degradation with TNCQ or $NOBF_4$. We theorize that while the reaction can proceed without an oxidant, CAN facilitates the oxidation of boranes, followed by the coordination of pinacol. Various alkyl- and halobenzenes were examined with optimized conditions, and we determined the resulting selectivity was highly dependent on the functional groups of the arene compounds. A few examples of our overall observations are that mono-substituted benzene compounds gave the corresponding aryl boronic esters with high *para* selectivity following the electronic control commonly observed in EAS reactions[49] (Figure 10B). Sterically bulkier alkyl groups also showed higher *para* selectivity in general. As we worked on a substrate scope, we observed a very unusual selectivity

for 1,3-disubstituted benzenes such as *m*-xylene. Unlike the previous electrophilic borylation examples, which showed selectivity for 4-positions (*ortho* to alkyl groups), substitution at 5-positions (*meta* to alkyl groups) was obtained with very high regioselectivity (Figure 10B). The two-step reaction approach of C-H borylation, followed by a cage deconstruction, eliminates the need for precious metals, sophisticated ligands, pre-functionalized boron reagents, or an inert atmosphere.

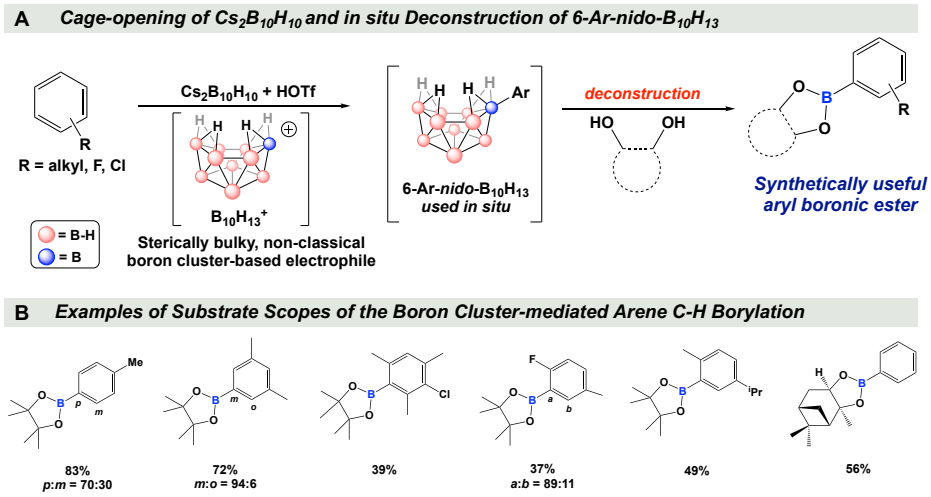

Figure 11. (A) - (B) Electrophilic borylation approach using *closo*-$[B_{10}H_{10}]^{2-}$ as a synthetic reagent. Figure 11A adapted from ref (49) with permission from Springer Nature.

Interestingly, a catalyst-free thermal arylation[50] used previously for *closo*-$[B_{12}H_{12}]^{2-}$ can be employed for direct arylation of *closo*-$[B_{10}H_{10}]^{2-}$, resulting in the formation of polyarylated clusters.[49] Oxidative deconstruction of these species leads to the isolation of mononuclear boronate ester molecules. It is worth noting that during the oxidation, a transient polyarylated cluster compound featuring a deep blue color and a diagnostic EPR signal consistent with the presence of a boron-centered radical can be observed. This example further showcases that a thermal arylation route could potentially circumvent some of the substrate limitations stemming from the use of the

strong acid in the electrophilic borylation and further shows the generality of oxidative cage deconstruction of arylated B_{10}-based species.

Conclusions and Outlook

Over the past decade, our work on functionalized and perfunctionalized boron clusters revealed a fascinating spectrum of redox activity and associated photophysical properties intricately tied to the specific redox states. As such, our group has explored these systems as unique molecular building blocks for a variety of applications. The exceptional electrochemical stability of numerous perfunctionalized $B_{12}(OR)_{12}$ clusters was demonstrated via a prototype symmetric flow cell setup, in which post-run analysis showed negligible decomposition of the active species (< 0.1%), even after electrochemical cycling between two oxidation states for 45 days. Another area our group is currently pursuing is the integration of these redox-active perfunctionalized clusters into extended solids to create new hybrid materials. In particular, we showed that one can use boron clusters as unique molecular cross-linkers to alter the photophysical properties of metal oxides. This work was also conceptually extended to several other hybrid systems, including conjugated polymers. Specifically, we demonstrated that by using redox-active cluster-based dopants, one could achieve an unprecedented level of conductivity in such hybrid systems. Due to their large steric profile, these boron cluster dopants spatially separate and electrostatically shield counterions from carriers, resulting in fully delocalized polarons. We continue to explore and understand these systems by further chemical modifications to the boron cluster core, as well as extending these principles to other boron cluster systems for integration into additional classes of materials. One recent example of such integration is our work showing how the $B_{12}(OCH_3)_{12}$ cluster can be electrochemically cycled in the solid state. Conceptually, the above studies showcase a fundamentally new theme in chemistry featuring photoredox-active molecules with switchable

weakly-coordinating anionic (WCA) behavior, where the identity of the functional groups grafted onto a perfunctionalized cluster can modulate the strength of interaction of the cluster with a cation, both in solution and in the solid state.

It is important to note that not all boron clusters exhibit reversible multi-electron redox properties, however. For example, our studies of functionalized *closo*-$[B_6H_6]^{2-}$ and, more recently, *closo*-$[B_{10}H_{10}]^{2-}$ species show that these compounds can undergo interesting cage rupture processes upon a single-electron oxidation from the 2- state. When this cage rupture occurs in the presence of chelating diols, this process can be ultimately harnessed and leveraged for a controlled cage deconstruction in the context of using the parent clusters as synthetic reagents. As a result of this oxidative deconstruction, exopolyhedral B-C bonds carrying an organic substituent can be preserved while cage B-B moieties break, delivering for the first time a convenient pathway for a clean disassembly of the polynuclear boron clusters into mononuclear alkyl- and aryl-based boronate esters commonly used in organic synthesis.

Conceptually, our work supports the notion that three-dimensional delocalized systems comprised of boron can stabilize various redox states. This observation is somewhat reminiscent of the work on perfunctionalized benzene-based scaffolds and draws several parallels regarding redox plasticity in both systems.[51-53] Our findings are also complimentary to the recent developments in the areas of redox-active polyhedral carboranes (boron clusters containing one or multiple carbon-based vertices),[54-61] as well as small mono- or dinuclear boron-based compounds,[62-66] which show broadly that various boron-atom containing architectures can undergo reversible redox events. Importantly, while we and others have shown that boron clusters can be strong chromophores, one should be cautious not to overgeneralize this concept. For example, due to their large HOMO-LUMO gaps, unfunctionalized boron clusters (e.g., *closo*-$[B_{12}H_{12}]^{2-}$) remain

photophysically inert. Therefore, they are energetically unlikely to engage in photoexcited charge-transfer or electron transfer behavior induced by visible light, despite some recent mechanistic claims.[67-68] We note that identification of impurities and careful and complete spectroscopic characterization is always critical to ascertain the photophysical properties of any molecular and hybrid systems containing new boron cluster species.[69-73]

Overall, it is becoming more and more apparent that the photophysical properties of three-dimensional aromatic boron clusters can be manipulated by judicious choice of functionalization chemistry, leading to a broad spectrum of properties, including photophysically inert systems on one extreme and the most powerful molecular photooxidants on the other. This remarkable spectrum of chemical tunability adds another dimension of complexity to the three-dimensional aromatic boron clusters and reinforces their "organomimetic" properties.[74]

Word Count: 4989

AUTHOR INFORMATION

Corresponding Author

***Alexander M. Spokoyny** - *Department of Chemistry and Biochemistry, University of California, Los Angeles, Los Angeles, California 90095, United States; California NanoSystems Institute, University of California, Los Angeles, Los Angeles, California 90095, United States*; https://orcid.org/0000-0002-5683-6240; E-mail: spokoyny@chem.ucla.edu.

Austin D. Ready - *Department of Chemistry and Biochemistry, University of California, Los Angeles, Los Angeles, California 90095, United States*; https://orcid.org/0000-0001-8051-7568.

Yessica A. Nelson - *Department of Chemistry and Biochemistry, University of California, Los Angeles, Los Angeles, California 90095, United States;* https://orcid.org/0000-0002-7744-051X.

Daniel F. Torres Pomares - *Department of Chemistry and Biochemistry, University of California, Los Angeles, Los Angeles, California 90095, United States*; https://orcid.org/0009-0007-7908-8648.

Acknowledgments

A. M. S. is grateful to all present and past co-workers and collaborators who have contributed to the projects described in this work. We thank NIH (NIGMS, R35GM124746), NSF (NSF CAREER, CHE-1846849), AFRL and DOE (SCALAR EFRC) for supporting projects in the laboratory over the past decade. A. M. S. is also grateful to the Sloan Foundation, Research Corporation for Science Advancement, and Dreyfus Foundation for individual fellowships and awards.

Notes

A.M. S. and several of his past co-workers are inventors on the patents for which they may receive royalty payments.

Biographies

Alexander M. Spokoyny received his Ph.D. in inorganic chemistry at Northwestern University in 2012. After an NIH-sponsored post-doctoral research fellowship stint at MIT working on chemical biology and bioorganometallic chemistry, Spokoyny started his independent career at UCLA Chemistry and Biochemistry in 2014. Over the past decade, Spokoyny and his laboratory have been interested in various fundamental and applied aspects of synthetic inorganic and organometallic chemistry, including redox-active boron-rich clusters.

Austin D. Ready is a Ph.D. candidate in inorganic chemistry at UCLA. He received a B.S. in chemistry from UC San Diego in 2019 working with Prof. Joshua Figueroa. His research focuses on the synthesis of dodecaborate-based clusters.

Yessica A. Nelson received her B.S. in chemistry from California State University, Los Angeles. She is an NSF GRFP fellow pursuing a Ph.D. in inorganic chemistry at UCLA focused on synthesizing vertex-differentiated boron-based clusters and related materials.

Daniel F. Torres Pomares is an undergraduate student at UCLA and a UC LEADS fellow. He plans to pursue a Ph.D. in chemistry, focusing on inorganic, organic, and therapeutic development.

References

(1) Wixtrom, A. I.; Shao, Y.; Jung, D.; Machan, C. W.; Kevork, S. N.; Qian, E. A.; Axtell, J. C.; Khan, S. I.; Kubiak, C. P.; Spokoyny, A. M. Rapid Synthesis of Redox-Active Dodecaborane $B_{12}(OR)_{12}$ Clusters Under Ambient Conditions. *Inorg. Chem. Frontiers* **2016**, *3*(5), 711–717, DOI: 10.1039/C5QI00263J.

(2) Axtell, J. C.; Messina, M. S.; Liu, J.-Y.; Galaktionova, D.; Schwan, J.; Porter, T. M.; Savage, M. D.; Wixtrom, A. I.; Rheingold, A. L.; Kubiak, C. P.; Winkler, J. R.; Gray, H. B.; Král, P.; Alexandrova, A. N.; Spokoyny, A. M. Photooxidative Generation of Dodecaborate-Based Weakly Coordinating Anions. Inorg. Chem. 2019, 58(16), 10516–10526, DOI: 10.1021/acs.inorgchem.9b00935.

(3) Mu, X.; Axtell, J. C.; Bernier, N. A.; Kirlikovali, K. O.; Jung, D.; Umanzor, A.; Qian, K.; Chen, X.; Bay, K. L.; Kirollos, M.; M.; Rheingold, A. L.; Houk, K. N.; Spokoyny, A. M.Sterically Unprotected Nucleophilic Boron Cluster Reagents. Chem 2019, 5(9), 2461–2469, DOI: 10.1016/j.chempr.2019.07.018.

(4) Ready, A. D.; Irshad, A.; Kallistova, A.; Carrillo, M.; Gembicky, M.; Seshadri, R.; Narayan, S.; Spokoyny, A. M. Electrochemical Cycling of Redox-Active Boron Cluster-Based Materials in the Solid State. J. Am. Chem. Soc. 2023, 145(26), 14345–14353, DOI: 10.1021/jacs.3c03065.

(5) Cai, Y.; Si, W.; Huang, W.; Chen, P.; Shao, J.; Dong, X. Organic Dye Based Nanoparticles for Cancer Phototheranostics. *Small* **2018**, *14*(25), 1704247, DOI: 10.1002/smll.201704247.

(6) Shirota, Y.; Kageyama, H., Organic Materials for Optoelectronic Applications: Overview. In *Handbook of Organic Materials for Electronic and Photonic Devices (Second Edition)*, Ostroverkhova, O., Ed. Woodhead Publishing: 2019; pp 3-42.

(7) Kamtekar, K. T.; Monkman, A. P.; Bryce, M. R. Recent Advances in White Organic Light-Emitting Materials and Devices (WOLEDs). *Adv. Mater* **2010**, *22*(5), 572–582, DOI: 10.1002/adma.200902148.

(8) Gsänger, M.; Bialas, D.; Huang, L.; Stolte, M.; Würthner, F. Organic Semiconductors based on Dyes and Color Pigments. *Adv. Mater* **2016**, *28*(19), 3615–3645, DOI: 10.1002/adma.201505440.

(9) King, R. B. Three-Dimensional Aromaticity in Polyhedral Boranes and Related Molecules. *Chem. Rev.* **2001**, *101*(5), 1119–1152, DOI: 10.1021/cr000442t.

(10) Kaim, W.; Hosmane, N. S.; Záliš, S.; Maguire, J. A.; Lipscomb, W. N. Boron Atoms as Spin Carriers in Two- and Three-Dimensional Systems. *Angew. Chem., Int. Ed.* **2009**, *48*(28), 5082–5091, DOI: 10.1002/anie.200803493.

(11) Lewis, J. S.; Kaczmarczyk, A. Polyhedral Borane Free Radicals. *J. Am. Chem. Soc.* **1966**, *88*(5), 1068–1069, DOI: 10.1021/ja00957a045.

(12) Klanberg, F.; Eaton, D. R.; Guggenberger, L. J.; Muetterties, E. L. Chemistry of Boranes. XXVIII. New Polyhedral Borane Anions, $B_8H_8^{2-}$, $B_8H_8^-$, and $B_7H_7^{2-}$. *Inorg. Chem.* **1967**, *6*(7), 1271–1281, DOI: 10.1021/ic50053a001.

(13) 1. Van, N.; Tiritiris, I.; Winter, R. F.; Sarkar, B.; Singh, P.; Duboc, C.; Muñoz-Castro, A.; Arratia-Pérez, R.; Kaim, W.; Schleid, T. Oxidative Perhydroxylation of [*closo*-$B_{12}H_{12}]^{2-}$ to the Stable Inorganic Cluster Redox System $[B_{12}(OH)_{12}]^{2-/\bullet-}$: Experiment and Theory. *Chem. Eur. J.* **2010**, *16*(37), 11242–11245, DOI: 10.1002/chem.201001374.

(14) Wiersema, R. J.; Middaugh, R. L. Electrochemical Oxidation of $B_{12}H_{12}^{2-}$. *J. Am. Chem. Soc.* **1967**, *89*(19), 5078–5078, DOI: 10.1021/ja00995a067.

(15) Wiersema, R. J.; Middaugh, R. L. Electrochemical Preparation and Halogenation of 1,1'-μ-hydro-bis(undecahydro-*closo*-dodecaborate)(3-), $B_{24}H_{23}^{3-}$. *Inorg. Chem.* **1969**, *8*(10), 2074–2079, DOI: 10.1021/ic50080a009.

(16) Peymann, T.; Knobler, C. B.; Hawthorne, M. F. An Unpaired Electron Incarcerated Within an Icosahedral Borane Cage: Synthesis and Crystal Structure of the Blue, Air-Stable {[*closo*-$B_{12}(CH_3)_{12}]^{\cdot}$}– Radical. *Chem. Commun.* **1999**, No. 20, 2039–2040, DOI: 10.1039/A905406E.

(17) Peymann, T.; Knobler, C. B.; Hawthorne, M. F. An Icosahedral Array of Methyl Groups Supported by an Aromatic Borane Scaffold: The [*closo*-$B_{12}(CH_3)_{12}]^{2-}$ Ion. *J. Am. Chem. Soc.* **1999**, *121*(23), 5601–5602, DOI: 10.1021/ja990884q.

(18) Peymann, T.; Herzog, A.; Knobler, C. B.; Hawthorne, M. F. Aromatic Polyhedral Hydroxyborates: Bridging Boron Oxides and Boron Hydrides. *Angew. Chem., Int. Ed.* **1999**, *38*(8), 1061–1064, DOI:10.1002/(SICI)1521-3773(19990419)38:8<1061::AID-ANIE1061>3.0.CO;2-B.

(19) Peymann, T.; Knobler, C. B.; Khan, S. I.; Hawthorne, M. F. Dodecahydroxy-*closo*-dodecaborate(2−). *J. Am. Chem. Soc.* **2001**, *123*(10), 2182–2185, DOI: 10.1021/ja0014887.

(20) Maderna, A.; Knobler, C. B.; Hawthorne, M. F. Twelvefold Functionalization of an Icosahedral Surface by Total Esterification of $[B_{12}(OH)_{12}]^{2-}$: 12(12)-Closomers. *Angew. Chem., Int. Ed.* **2001**, *40*(16), 2947–2947, DOI: 10.1002/1521-3773(20010817)40:16<2947::AID-ANIE33332947>3.0.CO;2-X.

(21) Li, T.; Jalisatgi, S. S.; Bayer, M. J.; Maderna, A.; Khan, S. I.; Hawthorne, M. F. Organic Syntheses on an Icosahedral Borane Surface: Closomer Structures with Twelvefold Functionality. *J. Am. Chem. Soc.* **2005**, *127*(50), 17832–17841, DOI: 10.1021/ja055226m.

(22) Peymann, T.; Knobler, C. B.; Khan, S. I.; Hawthorne, M. F. Dodeca(Benzyloxy)Dodecaborane, $B_{12}(OCH_2Ph)_{12}$: A Stable Derivative of hyper*closo*-$B_{12}H_{12}$. *Angew. Chem., Int. Ed.* **2001**, *40*(9), 1664–1667, DOI: 10.1002/1521-3773(20010504)40:9<1664::AID-ANIE16640>3.0.CO;2-O.

(23) Farha, O. K.; Julius, R. L.; Lee, M. W.; Huertas, R. E.; Knobler, C. B.; Hawthorne, M. F. Synthesis of Stable Dodecaalkoxy Derivatives of hyper*closo*- $B_{12}H_{12}$. *J. Am. Chem. Soc.* **2005**, *127*(51), 18243–18251, DOI: 10.1021/ja0556373.

(24) Wixtrom, A. I.; Parvez, Z. A.; Savage, M. D.; Qian, E. A.; Jung, D.; Khan, S. I.; Rheingold, A. L.; Spokoyny, A. M. Tuning the Electrochemical Potential of Perfunctionalized Dodecaborate Clusters Through Vertex Differentiation. *Chem. Commun.* **2018**, *54*(46), 5867–5870, DOI: 10.1039/C8CC03477J.

(25) Lee, M. W.; Farha, O. K.; Hawthorne, M. F.; Hansch, C. H. Alkoxy Derivatives of Dodecaborate: Discrete Nanomolecular Ions with Tunable Pseudometallic Properties. *Angew. Chem., Int. Ed.* **2007**, *46*(17), 3018–3022, DOI: 10.1002/anie.200605126.

(26) Schwan, J. L. Electronic Structure of Perfunctionalized Dodecaborate Clusters. Ph.D. Dissertation, California Institute of Technology, Pasadena, CA, 2020. https://resolver.caltech.edu/CaltechTHESIS:04062020-155127311 (accessed 2023-11-25)

(27) Aubry, T. J.; Axtell, J. C.; Basile, V. M.; Winchell, K. J.; Lindemuth, J. R.; Porter, T. M.; Liu, J.-Y.; Alexandrova, A. N.; Kubiak, C. P.; Tolbert, S. H.; Spokoyny, A.M.; Schwartz, B.J. Dodecaborane-Based Dopants Designed to Shield Anion Electrostatics Lead to Increased Carrier Mobility in a Doped Conjugated Polymer. *Adv. Mater.* **2019**, *31*(11), 1805647, DOI: 10.1002/adma.201805647.

(28) Aubry, T. J.; Winchell, K. J.; Salamat, C. Z.; Basile, V. M.; Lindemuth, J. R.; Stauber, J. M.; Axtell, J. C.; Kubena, R. M.; Phan, M. D.; Bird, M. J.; Spokoyny, A. M.; Tolbert, S.H.; Schwartz, B.J. Tunable Dopants with Intrinsic Counterion Separation Reveal the Effects of Electron Affinity on Dopant Intercalation and Free Carrier Production in Sequentially Doped Conjugated Polymer Films. *Adv. Funct. Mater.* **2020**, *30*(28), 2001800, DOI: 10.1002/adfm.202001800.

(29) Murrey, T. L.; Aubry, T. J.; Ruiz, O. L.; Thurman, K. A.; Eckstein, K. H.; Doud, E. A.; Stauber, J. M.; Spokoyny, A. M.; Schwartz, B. J.; Hertel, T.; Blackburn J.L.; Ferguson, A.J. Tuning Counterion Chemistry to Reduce Carrier Localization in Doped Semiconducting Carbon Nanotube Networks. *Cell Reports Physical Science* **2023**, *4*(5), 101407, DOI: 10.1016/j.xcrp.2023.101407.

(30) Hermosilla-Palacios, M. A.; Martinez, M.; Doud, E. A.; Hertel, T.; Spokoyny, A. M.; Cambré, S.; Wenseleers, W.; Kim, Y.-H.; Ferguson, A. J.; Blackburn, J. L. Carrier Density and Delocalization Signatures in Doped Carbon Nanotubes from Quantitative Magnetic Resonance. *Nanoscale Horizons* **2023**, DOI: 10.1039/D3NH00480E.

(31) Messina, M. S.; Axtell, J. C.; Wang, Y.; Chong, P.; Wixtrom, A. I.; Kirlikovali, K. O.; Upton, B. M.; Hunter, B. M.; Shafaat, O. S.; Khan, S. I.; Winkler, J.R.; Gray, H.B.; Alexandrova, A.N.; Maynard, H.D.; Spokoyny, A.M. Visible-Light-Induced Olefin Activation Using 3D Aromatic

Boron-Rich Cluster Photooxidants. *J. Am. Chem. Soc.* **2016**, *138*(22), 6952–6955, DOI: 10.1021/jacs.6b03568.

(32) Qian, E. A.; Wixtrom, A. I.; Axtell, J. C.; Saebi, A.; Jung, D.; Rehak, P.; Han, Y.; Moully, E. H.; Mosallaei, D.; Chow, S.; Messina, M.S.; Wang, J.Y.; Royappa, A.T.; Rheingold, A.L.; Maynard, H.D.; Král, P.; Spokoyny, A.M. Atomically Precise Organomimetic Cluster Nanomolecules Assembled via Perfluoroaryl-Thiol S_NAr Chemistry. *Nat. Chem.* **2017**, *9*(4), 333–340, DOI: 10.1038/nchem.2686.

(33) Stauber, J. M.; Qian, E. A.; Han, Y., Rheingold, A.L.; Král, P.; Fujita, D.; Spokoyny, A.M. An Organometallic Strategy for Assembling Atomically Precise Hybrid Nanomaterials. *J. Am. Chem. Soc*., **2020**, 142 (1), 327-334, DOI: 10.1021/jacs.9b10770.

(34) Barton, J. L.; Wixtrom, A. I.; Kowalski, J. A.; Qian, E. A.; Jung, D.; Brushett, F. R.; Spokoyny, A. M. Perfunctionalized Dodecaborate Clusters as Stable Metal-Free Active Materials for Charge Storage. *ACS Appl. Energy Mater.* **2019**, *2*(7), 4907–4913, DOI: 10.1021/acsaem.9b00610.

(35) Stauber, J. M.; Schwan, J.; Zhang, X.; Axtell, J. C.; Jung, D.; McNicholas, B. J.; Oyala, P. H.; Martinolich, A. J.; Winkler, J. R.; See, K. A.; Miller, T.F.; Gray, H.B.; Spokoyny, A.M. A Super-Oxidized Radical Cationic Icosahedral Boron Cluster. *J. Am. Chem. Soc.* **2020**, *142*(30), 12948–12953, DOI: 10.1021/jacs.0c06159.

(36) Li, B.; Zhang, X.; Stauber, J. M.; Miller, T. F.; Spokoyny, A. M. Electronic Structure of Superoxidized Radical Cationic Dodecaborate-Based Clusters. *J. Phys. Chem. A* **2021**, *125*(28), 6141–6150, DOI: 10.1021/acs.jpca.1c03927.

(37) Jung, D.; Saleh, L. M. A.; Berkson, Z. J.; El-Kady, M. F.; Hwang, J. Y.; Mohamed, N.; Wixtrom, A. I.; Titarenko, E.; Shao, Y.; McCarthy, K.; Guo, Jian; Martini, I.B.; Kraemer, S.; Wegener, E.C.; Saint-Cricq, P.; Ruehle, B.; Langeslay; R.R.; Delferro, M.; Brosmer, J.L.; Hendon, C.H.; Gallagher-Jones, M.; Rodriguez, J.; Chapman, K.W.; Miller, J.T.; Duan, X.; Kaner, R.B.; Zink, J.I.; Chmelka, B.F.; Spokoyny, A.M. A Molecular Cross-Linking Approach for Hybrid Metal Oxides. *Nat. Mater.* **2018**, *17*(4), 341–348, DOI: 10.1038/s41563-018-0021-9.

(38) Jung, D.; Muni, M.; Marin, G.; Ramachandran, R.; El-Kady, M. F.; Balandin, T.; Kaner, R. B.; Spokoyny, A. M. Enhancing Cycling Stability of Tungsten Oxide Supercapacitor Electrodes via a Boron Cluster-Based Molecular Cross-Linking Approach. *J. Mater. Chem. A* **2020**, *8*(35), 18015–18023, DOI: 10.1039/D0TA05915C.

(39) Kweon, K. E.; Varley, J. B.; Shea, P.; Adelstein, N.; Mehta, P.; Heo, T. W.; Udovic, T. J.; Stavila, V.; Wood, B. C. Structural, Chemical, and Dynamical Frustration: Origins of Superionic Conductivity in *closo*-Borate Solid Electrolytes. *Chem. Mater.* **2017**, *29*(21), 9142–9153, DOI: 10.1021/acs.chemmater.7b02902.

(40) Boeré, R. T.; Derendorf, J.; Jenne, C.; Kacprzak, S.; Keßler, M.; Riebau, R.; Riedel, S.; Roemmele, T. L.; Rühle, M.; Scherer, H.; Vent-Schmidt, T.; Warneke, J.; Weber, S. On the Oxidation of the Three-Dimensional Aromatics $[B_{12}X_{12}]^{2-}$ (X=F, Cl, Br, I). *Chem. Eur. J.* **2014**, *20*(15), 4447–4459, DOI: 10.1002/chem.201304405.

(41) Nelson, Y. A.; Irshad, A.; Kim, S.; Waddington, M. A.; Salamat, C. Z.; Gembicky, M.; Rheingold, A. L.; Carta, V.; Tolbert, S. H.; Narayan, S. R.; Spokoyny, A.M. Vertex Differentiation Strategy for Tuning the Physical Properties of *closo*-Dodecaborate Weakly Coordinating Anions. *Inorg. Chem.* **2023**, *62*(37), 15084–15093, DOI: 10.1021/acs.inorgchem.3c01992.

(42) Peymann, T.; Knobler, C. B.; Hawthorne, M. F. A Study of the Sequential Acid-Catalyzed Hydroxylation of Dodecahydro-*closo*-dodecaborate(2−). *Inorg. Chem.* **2000**, *39*(6), 1163–1170, DOI: 10.1021/ic991105+.

(43) Hansen, B. R. S.; Paskevicius, M.; Jørgensen, M.; Jensen, T. R. Halogenated Sodium-*closo*-Dodecaboranes as Solid-State Ion Conductors. *Chem. Mater.* **2017**, *29*(8), 3423–3430, DOI: 10.1021/acs.chemmater.6b04797.

(44) Jørgensen, M.; Jensen, S. R. H.; Humphries, T. D.; Rowles, M. R.; Sofianos, M. V.; Buckley, C. E.; Jensen, T. R.; Paskevicius, M. Hydroxylated *closo*-Dodecaborates $M_2B_{12}(OH)_{12}$ (M = Li, Na, K, and Cs); Structural Analysis, Thermal Properties, and Solid-State Ionic Conductivity. *J. Phys. Chem. C* **2020**, *124*(21), 11340–11349, DOI: 10.1021/acs.jpcc.0c02523.

(45) Preetz, W.; Peters, G. The Hexahydro-*closo*-hexaborate Dianion $[B_6H_6]^{2-}$ and Its Derivatives. *Eur. J. Inorg. Chem.* **1999**, *1999*(11), 1831–1846, DOI: 10.1002/(SICI)1099-0682(199911)1999:11<1831::AID-EJIC1831>3.0.CO;2-J.

(46) Axtell, J. C.; Kirlikovali, K. O.; Jung, D.; Dziedzic, R. M.; Rheingold, A. L.; Spokoyny, A. M. Metal-Free Peralkylation of the *closo*-Hexaborate Anion. *Organometallics* **2017**, *36*(6), 1204–1210, DOI: 10.1021/acs.organomet.7b00078.

(47) Hawthorne, M. F.; Mavunkal, I. J.; Knobler, C. B. Electrophilic Reactions of Protonated *closo*-$B_{10}H_{10}^{2-}$ with Arenes, Alkane Carbon-Hydrogen Bonds, and Triflate Ion Forming Aryl, Alkyl, and Triflate *nido*-6-X- $B_{10}H_{13}$ derivatives. *J. Am. Chem. Soc.* **1992**, *114*(11), 4427–4429, DOI: 10.1021/ja00037a074.

(48) Bondarev, O.; Sevryugina, Y. V.; Jalisatgi, S. S.; Hawthorne, M. F. Acid-Induced Opening of [*closo*-$B_{10}H_{10}]^{2-}$ as a New Route to 6-Substituted *nido*-$B_{10}H_{13}$ Decaboranes and Related Carboranes. *Inorg. Chem.* **2012**, *51*(18), 9935–9942, DOI: 10.1021/ic3014267.

(49) Kim, S.; Treacy, J. W.; Nelson, Y. A.; Gonzalez, J. A. M.; Gembicky, M.; Houk, K. N.; Spokoyny, A. M. Arene C–H Borylation Strategy Enabled by a Non-Classical Boron Cluster-Based Electrophile. *Nat. Commun.* **2023**, *14*(1), 1671, DOI: 10.1038/s41467-023-37258-6.

(50) Preetz, W.; von Bismarck, R. Darstellung, ^{11}B-, ^{13}C- und ^{1}H-NMR-Spektren von Halogenophenyl- und Phenyloxyhydrododecaboraten, $[(XC_6H_4)_nB_{12}H_{12-n}]^{2-}$ (X = Br, I; n = 1−3) und $[(C_6H_5O)B_{12}H_{11}]^{2-}$. *J. Organomet. Chem.* **1991**, *411*(1), 25–35, DOI: 10.1016/0022-328X(91)86003-9.

(51) Thomaides, J.; Przemyslaw, M.; Breslow, R. Electron-Rich Hexasubstituted Benzene Derivatives and their Oxidized Cation Radicals, Dications with Potential Triplet Ground States, and Polycations. *J. Am. Chem. Soc.* **1988**, *110*(12), 3970–3979, DOI: 10.1021/ja00220a040.

(52) Dixon, D. A.; Calabrese, J. C.; Miller, J. S. The Structure of Hexaaminobenzene. *Angew. Chem., Int. Ed.* **1989**, *28*(1), 90–92, DOI: 10.1002/anie.198900901.

(53) Han, Z.; Vaid, T. P.; Rheingold, A. L. Hexakis(4-(N-butylpyridylium))benzene: A Six-Electron Organic Redox System. *J. Org. Chem.* **2008**, *73*(2), 445–450, DOI: 10.1021/jo701944c.

(54) Miller, J. R.; Cook, A. R.; Šimková, L.; Pospíšil, L.; Ludvík, J.; Michl, J. The Impact of Huge Structural Changes on Electron Transfer and Measurement of Redox Potentials: Reduction of ortho-12-Carborane. *J. Phys. Chem. B* **2019**, *123*(45), 9668–9676, DOI: 10.1021/acs.jpcb.9b08151.

(55) Nussbaum, B. C.; Humphries, A. L.; Gange, G. B.; Peryshkov, D. V. Redox-Active Carborane Clusters in Bond Activation Chemistry and Ligand Design. *Chem. Commun.* **2023**, *59*(66), 9918–9928, DOI: 10.1039/D3CC03011C.

(56) Keener, M.; Hunt, C.; Carroll, T. G.; Kampel, V.; Dobrovetsky, R.; Hayton, T. W.; Ménard, G. Redox-Switchable Carboranes for Uranium Capture and Release. *Nature* **2020**, *577*(7792), 652–655, DOI: 10.1038/s41586-019-1926-4.

(57) Yao, S.; Kostenko, A.; Xiong, Y.; Ruzicka, A.; Driess, M. Redox Noninnocent Monoatomic Silicon(0) Complex ("Silylone"): Its One-Electron-Reduction Induces an Intramolecular One-Electron-Oxidation of Silicon(0) to Silicon(I). *J. Am. Chem. Soc.* **2020**, *142*(29), 12608–12612, DOI: 10.1021/jacs.0c06238.

(58) Kahlert, J.; Stammler, H.-G.; Neumann, B.; Harder, R. A.; Weber, L.; Fox, M. A. Crystal Structures of the Carborane Dianions $[1,4\text{-}(PhCB_{10}H_{10}C)_2C_6H_4]^{2-}$ and $[1,4\text{-}(PhCB_{10}H_{10}C)_2C_6F_4]^{2-}$ and the Stabilizing Role of the *para*-Phenylene Unit on 2 *n*+3 Skeletal Electron Clusters. *Angew. Chem., Int. Ed.* **2014**, *53*(14), 3702–3705, DOI: 10.1002/anie.201310718.

(59) Körbe, S.; Schreiber, P. J.; Michl, J. Chemistry of the Carba-*closo*-dodecaborate(−) Anion, $CB_{11}H_{12}^-$. *Chem. Rev.* **2006**, *106*(12), 5208–5249, DOI: 10.1021/cr050548u.

(60) Zhang, J.; Xie, Z. Synthesis, Structure, and Reactivity of 13- and 14-Vertex Carboranes. *Acc. Chem. Res.* **2014**, *47*(5), 1623–1633, DOI: 10.1021/ar500091h.

(61) Fisher, S. P.; Tomich, A. W.; Lovera, S. O.; Kleinsasser, J. F.; Guo, J.; Asay, M. J.; Nelson, H. M.; Lavallo, V. Nonclassical Applications of *closo*-Carborane Anions: From Main Group Chemistry and Catalysis to Energy Storage. *Chem. Rev.* **2019**, *119*(14), 8262–8290, DOI: 10.1021/acs.chemrev.8b00551.

(62) Légaré, M.-A.; Pranckevicius, C.; Braunschweig, H. Metallomimetic Chemistry of Boron. *Chem. Rev.* **2019**, *119*(14), 8231–8261, DOI: 10.1021/acs.chemrev.8b00561.

(63) Su, Y.; Kinjo, R. Boron-Containing Radical Species. *Coord. Chem. Rev.* **2017**, *352*, 346–378, DOI: 10.1016/j.ccr.2017.09.019.

(64) Hertz, V. M.; Bolte, M.; Lerner, H.-W.; Wagner, M. Boron-Containing Polycyclic Aromatic Hydrocarbons: Facile Synthesis of Stable, Redox-Active Luminophores. *Angew. Chem., Int. Ed.* **2015**, *54*(30), 8800–8804, DOI: 10.1002/anie.201502977.

(65) Wong, A.; Chu, J.; Wu, G.; Telser, J.; Dobrovetsky, R.; Ménard, G. Redox-Controlled Reactivity at Boron: Parallels to Frustrated Lewis/Radical Pair Chemistry. *Inorg. Chem.* **2020**, *59*(14), 10343–10352, DOI: 10.1021/acs.inorgchem.0c01464.

(66) Litters, S.; Kaifer, E.; Himmel, H.-J. A Radical Tricationic Rhomboid Tetraborane(4) with Four-Center, Five-Electron Bonding. *Angew. Chem., Int. Ed.* **2016**, *55*(13), 4345–4347, DOI: 10.1002/anie.201600296.

(67) Zhao, X.; Chen, H.; Li, H.; Hu, B.; Kuklin, A. V.; Baryshnikov, G. V.; Ågren, H.; Hu, W.; Hu, G.; Zhou, X.; Zhang, H. Persistent Radical Pairs Trigger Nano-Gold to Highly Efficiently and Highly Selectively Drive the Value-Added Conversion of Nitroaromatics. *Chem. Catal.* **2021**, *1*(5), 1118–1132. DOI: 10.1016/j.checat.2021.08.017.

(68) Li, W.-Z.; Chen, H.; Shen, M.-N.; Yang, Z.; Fan, Z.; Xiao, J.; Chen, J.; Zhang, H.; Wang, Z.; Wang, X.-Q. Chaotropic Effect Stabilized Radical-Containing Supramolecular Organic Frameworks for Photothermal Therapy. *Small* **2022**, *18*(15), 2108055, DOI: 10.1002/smll.202108055.

(69) Mukherjee, S.; Thilagar, P. Boron clusters in luminescent materials. *Chem. Commun.* **2016**, *52*(6), 1070–1093, DOI: 10.1039/C5CC08213G.

(70) Kunkely, H.; Vogler, A. Is *o*-Carborane Photoluminescent? *Inorg. Chim. Acta* **2004**, *357*(15), 4607–4609, DOI: 10.1016/j.ica.2004.05.039.

(71) Teprovich, J. A.; Colón-Mercado, H.; Ii, A. L. W.; Ward, P. A.; Greenway, S.; Missimer, D. M.; Hartman, H.; Velten, J.; Christian, J. H.; Zidan, R. Bi-Functional $Li_2B_{12}H_{12}$ for Energy Storage and Conversion Applications: Solid-State Electrolyte and Luminescent Down-Conversion Dye. *J. Mater. Chem. A* **2015**, *3*(45), 22853–22859, DOI:10.1039/C5TA06549F.

(72) Paskevicius, M.; Jakobsen, A. S.; Bregnhøj, M.; Hansen, B. R. S.; Møller, K. T.; Ogilby, P. R.; Jensen, T. R. Comment on "Bi-Functional $Li_2B_{12}H_{12}$ for Energy Storage and Conversion Applications: Solid-State Electrolyte and Luminescent Down-Conversion Dye" by J. A. Teprovich Jr, H. Colón-Mercado, A. L. Washington II, P. A. Ward, S. Greenway, D. M. Missimer, H. Hartman, J. Velten, J. H. Christian and R. Zidan, *J. Mater. Chem*. A, **2015**, 3, 22853. *J. Mater. Chem. A* **2019**, *7*(8), 4185–4187, DOI: 10.1039/C8TA10735A.

(73) Teprovich, J. A.; Zidan, R. Reply to the 'Comment on "Bi-Functional $Li_2B_{12}H_{12}$ for Energy Storage and Conversion Applications: Solid-State Electrolyte and Luminescent Down-Conversion Dye"' by M. Paskevicius, A. S. Jakobsen, M. Bregnhøj, B. R. S. Hansen, K. T. Møller, P. R. Ogilby and T. R. Jensen, J. Mater. Chem. A., 2019, DOI: 10.1039/c8ta10735a. *J. Mater. Chem. A* **2019**, *7*(8), 4188–4189, DOI: 10.1039/C9TA00407F.

(74) Spokoyny, A. M. New Ligand Platforms Featuring Boron-Rich Clusters as Organomimetic Substituents. *Pure Appl. Chem.* **2013**, *85*(5), 903–919, DOI: 10.1351/PAC-CON-13-01-13.

Graphical Abstract (TOC):